Fast and stable multivariate kernel density estimation by fast sum updating

Nicolas Langrené, Xavier Warin

Fast and stable multivariate kernel density estimation by fast sum updating

Nicolas Langrené*, Xavier Warin†

First version: December 5, 2017
This version: October 22, 2018

Accepted for publication in the
Journal of Computational and Graphical Statistics

Kernel density estimation and kernel regression are powerful but computationally expensive techniques: a direct evaluation of kernel density estimates at M evaluation points given N input sample points requires a quadratic $\mathcal{O}(MN)$ operations, which is prohibitive for large scale problems. For this reason, approximate methods such as binning with Fast Fourier Transform or the Fast Gauss Transform have been proposed to speed up kernel density estimation. Among these fast methods, the Fast Sum Updating approach is an attractive alternative, as it is an exact method and its speed is independent of the input sample and the bandwidth. Unfortunately, this method, based on data sorting, has for the most part been limited to the univariate case. In this paper, we revisit the fast sum updating approach and extend it in several ways. Our main contribution is to extend it to the general multivariate case for general input data and rectilinear evaluation grid. Other contributions include its extension to a wider class of kernels, including the triangular, cosine and Silverman kernels, its combination with parsimonious additive multivariate kernels, and its combination with a fast approximate k-nearest-neighbors bandwidth for multivariate datasets. Our numerical tests of multivariate regression and density estimation confirm the speed, accuracy and stability of the method. We hope this paper will renew interest for the fast sum updating approach and help solve large-scale practical density estimation and regression problems.

Keywords: adaptive bandwidth; fast k-nearest-neighbors; fast kernel density estimation; fast kernel regression; fast kernel summation; balloon bandwidth; multivariate partition; fast convolution

MSC codes: 62G07; 62G08; 65C60; **ACM codes**: G.3; F.2.1; G.1.0

*CSIRO Data61, RiskLab Australia, nicolas.langrene@csiro.au
†EDF R&D, FiME (Laboratoire de Finance des Marchés de l'Énergie), warin@edf.fr

1. Introduction

Let $(x_1, y_1), (x_2, y_2), \ldots, (x_N, y_N)$ be a sample of N input points x_i and output points y_i drawn from a joint distribution (X, Y). The kernel density estimator (aka Parzen-Rosenblatt estimator) of the density of X at the evaluation point z is given by:

$$\hat{f}_{\mathrm{KDE}}(z) := \frac{1}{N} \sum_{i=1}^{N} K_h(x_i - z) \tag{1}$$

where $K_h(u) := \frac{1}{h} K\left(\frac{u}{h}\right)$ with kernel K and bandwidth h. The Nadaraya-Watson kernel regression estimator of $\mathbb{E}\left[Y \,|X = z\right]$ is given by:

$$\hat{f}_{\mathrm{NW}}(z) := \frac{\sum_{i=1}^{N} K_h(x_i - z) y_i}{\sum_{i=1}^{N} K_h(x_i - z)} \tag{2}$$

The estimator $\hat{f}_{\mathrm{NW}}(z)$ performs a kernel-weighted local average of the response points y_i that are such that their corresponding inputs x_i are close to the evaluation point z. It can be described as a locally constant regression. More generally, locally linear regressions can be performed:

$$\hat{f}_{\mathrm{L}}(z) := \min_{\alpha(z), \beta(z)} \sum_{i=1}^{N} K_h(x_i - z) \left[y_i - \alpha(z) - \beta(z) x_i\right]^2 \tag{3}$$

In this case, a weighted linear regression is performed for each evaluation point z This formulation can be generalized to quadratic and higher-order local polynomial regressions.

Discussions about the properties and performance of these classical kernel smoothers (1)-(2)-(3) can be found in various textbooks, such as Loader (1999), Härdle et al. (2004), Hastie et al. (2009) and Scott (2014).

The well known computational problem with the implementation of the kernel smoothers (1)-(2)-(3) is that their direct evaluation on a set of M evaluation points requires $\mathcal{O}(M \times N)$ operations. In particular, when the evaluation points coincide with the input points $x_1, x_2, \ldots, x_N$, a direct evaluation requires a quadratic $\mathcal{O}(N^2)$ number of operations. To cope with this computational limitation, several approaches have been proposed over the years.

Data binning consists in summarizing the input sample into a set of equally spaced bins, so as to compute the kernel smoothers more quickly on the binned data. This data preprocessing allows for significant speedup, either by Fast Fourier Transform (Wand (1994), Gramacki and Gramacki (2017)) or by direct computation, see Silverman (1982), Scott (1985), Fan and Marron (1994), Turlachand and Wand (1996), Bowman and Azzalini (2003).

The *fast sum updating* method is based on the sorting of the input data and on a translation of the kernel from one evaluation point to the next, updating only the input points which do not belong to the intersection of the bandwidths of the two evaluation points, see Gasser and Kneip (1989), Seifert et al. (1994), Fan and Marron (1994), Werthenbach and Herrmann (1998), Chen (2006).

The *Fast Gauss Transform*, also known as Fast Multipole Method, is based on the expansion of the Gaussian kernel to disentangle the input points from the evaluation points and speed up the evaluation of the resulting sums, see Greengard and Strain (1991), Greengard and Sun (1998), Lambert et al. (1999), Yang et al. (2003), Morariu et al. (2009), Raykar et al. (2010), Sampath et al. (2010), Spivak et al. (2010).

The *dual-tree* method is based on space partitioning trees for both the input sample and the evaluation points. These tree structures are then used to compute distances between input points and evaluation points more quickly, see Gray and Moore (2001), Gray and Moore (2003), Lang et al. (2005), Lee et al. (2006), Ram et al. (2009), Curtin et al. (2013), Griebel and Wissel (2013), Lee et al. (2014).

Among all these methods, the fast sum updating is the only one which is exact (no extra approximation is introduced) and whose speed is independent of the input data, the kernel and the bandwidth. Its main drawback is that the required sorting of the input points has mostly limited this literature to the univariate case. Werthenbach and Herrmann (1998) attempted to extend the method to the bivariate case, under strong limitations, namely rectangular input sample, evaluation grid and kernel support.

In this paper, we revisit the fast sum updating approach and extend it to the general multivariate case. This extension requires a rectilinear evaluation grid and kernels with box support, but has no restriction on the input sample and can accommodate adaptive bandwidths. Moreover, it maintains the desirable properties of the fast sum updating approach, making it, so far, the only fast and exact algorithm for multivariate kernel smoothing under general input sample and general bandwidth.

2. Fast sum updating

2.1. Univariate case

In this section, we recall the fast sum updating algorithm in the univariate case. Let (x_1, y_1), (x_2, y_2),…,(x_N, y_N) be a sample of N input (source) points x_i and output points y_i, and let $z_1, z_2, \dots, z_M$ be a set of M evaluation (target) points. We first sort the input points and evaluation points: $x_1 \leq x_2 \leq \dots \leq x_N$ and $z_1 \leq z_2 \leq \dots \leq z_M$. In order to compute the kernel density estimator (1), the kernel regression (2) and the locally linear regression (3) for every evaluation point z_j, one needs to compute sums of the type

$$\mathbf{S}_j = \mathbf{S}_j^{p,q} := \frac{1}{N}\sum_{i=1}^{N} K_h(x_i - z_j) x_i^p y_i^q = \frac{1}{Nh}\sum_{i=1}^{N} K\left(\frac{x_i - z_j}{h}\right) x_i^p y_i^q \,, p = 0, 1,\ q = 0, 1 \qquad (4)$$

for every $j \in \{1, 2, \dots, M\}$. The direct, independent evaluation of these sums would require $\mathcal{O}(N \times M)$ operations (a sum of N terms for each $j \in \{1, 2, \dots, M\}$). The idea of fast sum updating is to use the information from the sum $\mathbf{S}_j$ to compute the next sum $\mathbf{S}_{j+1}$ without going through all the N input points again. We illustrate the idea with the Epanechnikov (parabolic) kernel $K(u) = \frac{3}{4}(1 - u^2)\mathbb{1}\{|u| \leq 1\}$. With this choice of kernel:

$$\begin{aligned}
\mathbf{S}_j^{p,q} &= \frac{1}{Nh}\sum_{i=1}^{N}\frac{3}{4}\left(1 - \left(\frac{x_i - z_j}{h}\right)^2\right) x_i^p y_i^q \mathbb{1}\{z_j - h \leq x_i \leq z_j + h\} \\
&= \frac{1}{Nh}\frac{3}{4}\sum_{i=1}^{N}\left(1 - \frac{z_j^2}{h^2} + 2\frac{z_j}{h^2}x_i - \frac{1}{h^2}x_i^2\right) x_i^p y_i^q \mathbb{1}\{z_j - h \leq x_i \leq z_j + h\} \\
&= \frac{3}{4Nh}\left\{\left(1 - \frac{z_j^2}{h^2}\right)\mathcal{S}^{p,q}([z_j - h, z_j + h]) + 2\frac{z_j}{h^2}\mathcal{S}^{p+1,q}([z_j - h, z_j + h]) - \frac{1}{h^2}\mathcal{S}^{p+2,q}([z_j - h, z_j + h])\right\}
\end{aligned} \qquad (5)$$

where

$$\mathcal{S}^{p,q}([L,R]) := \sum_{i=1}^{N} x_i^p y_i^q \mathbb{1}\{L \leq x_i \leq R\} \tag{6}$$

These sums $\mathcal{S}^{p,q}([z_j-h, z_j+h])$ can be evaluated quickly from $j=1$ to $j=M$ as long as the input points x_i and the evaluation points z_j are sorted in increasing order. Indeed,

$$\begin{aligned}
&\mathcal{S}^{p,q}([z_{j+1}-h, z_{j+1}+h]) = \sum_{i=1}^{N} x_i^p y_i^q \mathbb{1}\{z_{j+1}-h \leq x_i \leq z_{j+1}+h\} \\
&= \sum_{i=1}^{N} x_i^p y_i^q \mathbb{1}\{z_j-h \leq x_i \leq z_j+h\} \\
&- \sum_{i=1}^{N} x_i^p y_i^q \mathbb{1}\{z_j-h \leq x_i < z_{j+1}-h\} + \sum_{i=1}^{N} x_i^p y_i^q \mathbb{1}\{z_j+h < x_i \leq z_{j+1}+h\} \\
&= \mathcal{S}^{p,q}([z_j-h, z_j+h]) - \mathcal{S}^{p,q}([z_j-h, z_{j+1}-h[) + \mathcal{S}^{p,q}(]z_j+h, z_{j+1}+h])
\end{aligned} \tag{7}$$

Therefore one can simply update the sum $\mathcal{S}^{p,q}([z_j-h, z_{j+1}+h])$ for the evaluation point z_j to obtain the next sum $\mathcal{S}^{p,q}([z_{j+1}-h, z_{j+1}+h])$ for the next evaluation point z_{j+1} by subtracting the terms $x_i^p y_i^q$ for which x_i lie between z_j-h and $z_{j+1}-h$, and adding the terms $x_i^p y_i^q$ for which x_i lie between z_j+h and $z_{j+1}+h$. This can be achieved in a fast $\mathcal{O}(M+N)$ operations by going through the input points x_i, stored in increasing order at a cost of $\mathcal{O}(N \log N)$ operations, and through the evaluation points z_j, stored in increasing order at a cost of $\mathcal{O}(M \log M)$ operations. Algorithm 1 summarizes the whole procedure to compute equations (1), (2) and (3) in the case of the Epanechnikov kernel.

In the case of the Epanechnikov kernel, the expansion of the quadratic term $\left(\frac{x_i-z_j}{h}\right)^2$ separates the sources x_i from the targets z_j (equation (5)), which makes the fast sum updating approach possible. Such a separation occurs with other classical kernels as well, including the rectangular kernel, the triangular kernel, the cosine kernel and the Silverman kernel. Table 1 provides a list of ten kernels for which fast sum updating can be implemented, and Appendix A provides the detail of the updating formulas for these kernels. While most of these kernels have finite support $[-1,1]$, some such as the Laplacian kernel and Silverman kernel have infinite support. Not every kernel admits such a separation between sources and targets, the most prominent example being the Gaussian kernel $K(u) = \frac{1}{\sqrt{2\pi}} \exp(-u^2/2)$, for which the cross term $\exp(x_i z_j/h)$ cannot be split between one source term (depending on i only) and one target term (depending on j only). Approximating the cross-term to obtain such a separation is the path followed by the Fast Gauss Transform approach (Greengard and Strain (1991)).

While any kernel in Table 1 can be used for fast sum updating, we choose to use for the rest of the paper the Epanechnikov kernel $K(u) = \frac{3}{4}(1-u^2)\mathbb{1}\{|u| \leq 1\}$ for two reasons: this popular kernel is optimal in the sense that it minimizes the asymptotic mean integrated squared error (cf. Epanechnikov (1969)), and it supports fast sum updating with adaptive bandwidth $h = h_i$ or $h = h_j$ (see Algorithm 1, Appendix A and subsection 3.2).

Algorithm 1: Fast univariate kernel smoothing

Input:

X: sorted vector of N inputs $X[1] \leq \ldots \leq X[N]$
Y: vector of N outputs $Y[1], \ldots, Y[N]$
Z: sorted vector of M evaluation points $Z[1] \leq \ldots \leq Z[M]$
H: vector of M bandwidths $H[1], \ldots, H[M]$
▷ Z and H should be such that the vectors Z-H and Z+H are increasing

iL = 1 ▷ The indices $1 \leq iL \leq iR \leq N$ will be such that the current
iR = 1 ▷ bandwidth $[Z[m] - H[m], Z[m] + H[m]]$ contains the points $X[iL], X[iL+1], \ldots, X[iR]$
S$[p_1, p_2]$ = 0, $p_1 = 0, 1, \ldots, 4$, $p_2 = 0, 1$ ▷ Will contain the sum $\sum_{i=iL}^{iR} X[i]^{p_1} \times Y[i]^{p_2}$

for $m = 1, ..., M$ **do**
  while *(iR≤N) and (X[iR]<(Z[m]+H[m]))* **do**
    S$[p_1, p_2]$ = S$[p_1, p_2]$ + X[iR]^{p_1}×Y[iR]^{p_2} , $p_1 = 0, 1, \ldots, 4, p_2 = 0, 1$
    iR = iR + 1
  end
  while *(iL≤N) and (X[iL]<(Z[m]-H[m]))* **do**
    S$[p_1, p_2]$ = S$[p_1, p_2]$ − X[iL]^{p_1}×Y[iL]^{p_2} , $p_1 = 0, 1, \ldots, 4, p_2 = 0, 1$
    iL = iL + 1
  end
  ▷ Here S$[p_1, p_2]$=$\sum_{i=iL}^{iR} X[i]^{p_1} Y[i]^{p_2}$, which can be used to compute
  ▷ SK$[p_1, p_2]$=$\sum_{i=iL}^{iR} X[i]^{p_1} Y[i]^{p_2}\ K(Z[m], X[i])$
  C0 = 1.0 − Z[m]^2/H[m]^2; C1 = 2.0 × Z[m]/H[m]^2; C2 = 1/H[m]^2
  SK$[p_1, p_2]$ = C0×S$[p_1, p_2]$ + C1×S$[p_1 + 1, p_2]$ − C2×S$[p_1 + 2, p_2]$
  D[m] = 0.75×SK[0,0]/(H[m]×N)
  R0[m] = SK[0,1]/SK[0,0]
  $$\text{R1[m]}=\left[\begin{array}{cc} 1 & \text{Z[m]} \end{array}\right] \left[\begin{array}{cc} \text{SK}[0,0] & \text{SK}[1,0] \\ \text{SK}[1,0] & \text{SK}[2,0] \end{array}\right]^{-1} \left[\begin{array}{c} \text{SK}[0,1] \\ \text{SK}[1,1] \end{array}\right]$$
end
return D, R0, R1

Output:

D[m]: kernel density estimate of X
R0[m]: locally constant regression of Y on X (kernel regression)
R1[m]: locally linear regression of Y on X
▷ The three estimates D[m], R0[m] and R1[m] are evaluated at point Z[m] with bandwidth H[m] and Epanechnikov kernel, for each m=1,... ,M

Kernels compatible with fast sum updating

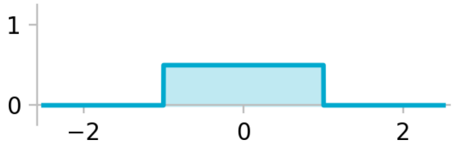

Rectangular (uniform)

$K(u) = \frac{1}{2}\mathbb{1}\{|u| \leq 1\}$

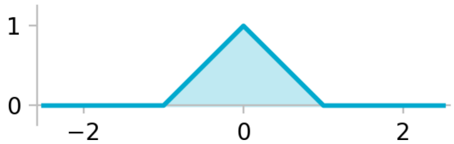

Triangular

$K(u) = (1 - |u|)\mathbb{1}\{|u| \leq 1\}$

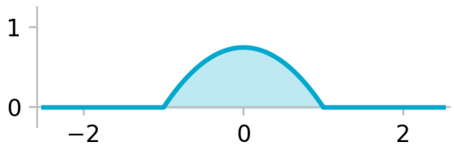

Parabolic (Epanechnikov)

$K(u) = \frac{3}{4}(1 - u^2)\mathbb{1}\{|u| \leq 1\}$

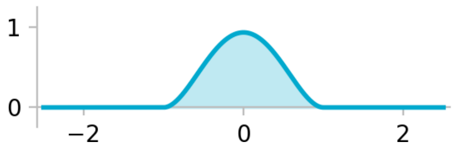

Biweight (Quartic)

$K(u) = \frac{15}{16}(1 - u^2)^2\mathbb{1}\{|u| \leq 1\}$

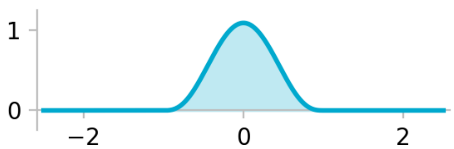

Triweight

$K(u) = \frac{35}{32}(1 - u^2)^3\mathbb{1}\{|u| \leq 1\}$

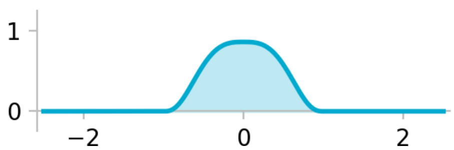

Tricube

$K(u) = \frac{70}{81}(1 - |u|^3)^3\mathbb{1}\{|u| \leq 1\}$

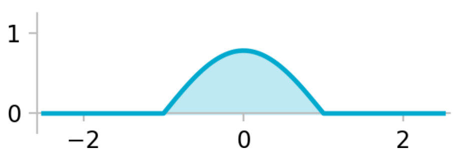

Cosine

$K(u) = \frac{\pi}{4}\cos\left(\frac{\pi}{2}u\right)\mathbb{1}\{|u| \leq 1\}$

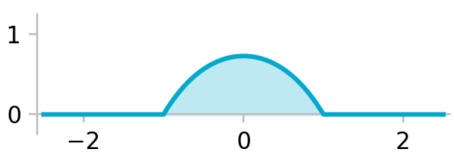

Hyperbolic cosine

$K(u) = \frac{1}{4 - 2\frac{\sinh(\log(2+\sqrt{3}))}{\log(2+\sqrt{3})}}\left\{2 - \cosh(\log(2+\sqrt{3})u)\right\}\mathbb{1}\{|u| \leq 1\}$

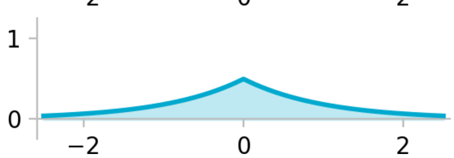

Laplacian

$K(u) = \frac{1}{2}\exp(-|u|)$

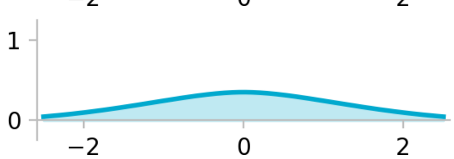

Silverman

$K(u) = \frac{1}{2}\exp\left(-\frac{|u|}{\sqrt{2}}\right)\sin\left(\frac{|u|}{\sqrt{2}} + \frac{\pi}{4}\right)$

Table 1: Kernels compatible with fast sum updating

2.2. Numerical stability

In Seifert et al. (1994), the direct fast sum updating approach described in Algorithm 1 was discarded for numerical stability reasons. With floating-point arithmetic, the difference $(x + y) - x$ is in general equal to $y \pm \varepsilon$, where ε corresponds to the floating point rounding error. In addition, the greater the scale difference between two floating numbers x and y, the greater the rounding error when computing $x + y$. Consequently, adding and subtracting N numbers in sequence has a worst-case rounding error that grows proportional to N.

In this paper, we argue that the advances in floating-point accuracy and stable floating-point summation in the past decades have made the direct fast sum updating approach viable and immune to numerical error. In addition to simple precautions such as normalization of input data and use of accurate floating-point formats such as quadruple-precision floating-point, a long list of stable summation algorithms have been proposed in the past fifty years, see among others Møller (1965), Kahan (1965), Linnainmaa (1974), Priest (1991) Higham (1993), Demmel and Hida (2003), McNamee (2004) and Boldo et al. (2017). The usual idea is to keep track of the current amount of floating-point rounding error, and to propagate it when adding new terms in the sum. Recently, a number of exact summation algorithms have been proposed, see Rump et al. (2008), Pan et al. (2009), Zhu and Hayes (2010) and Neal (2015). These algorithms are exact in the sense that the final result is the closest floating-point number, within the precision of the chosen floating-point format, to the exact mathematical sum of the inputs. Importantly, the computational complexity of exact summation remains linear in the number N of data points to sum. For example, for the recent Neal (2015), exact summation is less than a factor two slower than naive summation.

To sum up, with little modification, fast sum updating algorithms such as Algorithm 1 and its multivariate version 3 can be made completely immune to numerical instability. As a simple illustration, Algorithm 5 in Appendix shows how to combine Algorithm 3 with the stable Møller-Kahan summation algorithm (Møller (1965)). For simplicity and clarity, the fast sum updating algorithms presented in this paper omit the stabilisation components. All of them can be implemented with perfect numerical stability using the stable summation algorithms mentioned in this subsection.

2.3. Multivariate case

We now turn to the multivariate case. Let d be the dimension of the inputs. We consider again a sample $(x_1, y_1), (x_2, y_2), \ldots, (x_N, y_N)$ of N input points x_i and output points y_i, where the input points are now multivariate:

$$x_i = (x_{1,i}, x_{2,i}, \ldots, x_{d,i}) \ , \ i \in \{1, 2, \ldots, N\}$$

2.3.1. Multivariate kernel smoothers

The kernel smoothers (1), (2) and (3) can be extended to the multivariate case. A general form for a multivariate kernel is $K_{d,H}(u) = |H|^{-1/2} K_d(H^{-1/2}u)$, where $u = (u_1, u_2, \ldots, u_d) \in \mathbb{R}^d$ and where H is a symmetric positive definite $d \times d$ bandwidth matrix (see Wand and Jones (1995) for example). The eigenvalue decomposition of H yields $H = R\Delta^2 R^\top$ where R is a rotation matrix and $\Delta = \mathrm{diag}(h)$ is a diagonal matrix with strictly positive diagonal elements $h = (h_1, h_2, \ldots, h_d) \in \mathbb{R}^d$. Therefore, without loss of generality, one can focus on the diagonal bandwidth case $K_{d,h}(u) = \frac{1}{\Pi_{k=1}^d h_k} K_d(\frac{u_1}{h_1}, \frac{u_2}{h_2}, \ldots, \frac{u_d}{h_d})$ after a rotation of the input points x_i and the evaluation points z_j using R. Subsection 3.1 will discuss the choice of data rotation and subsection 2.3.3 will discuss the possible choices of multivariate kernels K_d compatible with fast sum updating. One can show (cf. Appendix C) that the computation of the multivariate version of the kernels smoothers (1), (2) and (3) boils down to the computation of the following sums:

$$\begin{aligned}\mathbf{S}_j &= \mathbf{S}^{p_1,p_2,q}_{k_1,k_2,j} := \frac{1}{N}\sum_{i=1}^N K_{d,h}(x_i - z_j) x^{p_1}_{k_1,i} x^{p_2}_{k_2,i} y_i^q \\ &= \frac{1}{N\Pi_{k=1}^d h_k} \sum_{i=1}^N K_d\left(\frac{x_{1,i}-z_{1,j}}{h_1}, \frac{x_{2,i}-z_{2,j}}{h_2}, \ldots, \frac{x_{d,i}-z_{d,j}}{h_d}\right) x^{p_1}_{k_1,i} x^{p_2}_{k_2,i} y_i^q \end{aligned} \tag{8}$$

for each evaluation point $z_j = (z_{1,j}, z_{2,j}, \ldots, z_{d,j}) \in \mathbb{R}^d$, $j \in \{1, 2, \ldots, M\}$, for powers $p_1, p_2, q = 0, 1$ and for dimension indices $k_1, k_2 = 1, 2, \ldots, d$.

Before expanding the sum (8) as was done in (5) in the univariate case, we first introduce the two conditions required for fast multivariate sum updating (subsection 2.3.2) and then discuss the choice of multivariate kernel (subsection 2.3.3).

2.3.2. Conditions

In order to extend the fast sum updating algorithm to the multivariate case, we require the following two conditions:

Condition 1. [Evaluation grid] We require the evaluation grid to be rectilinear, i.e., the M evaluation points $z_1, z_2, \ldots, z_M$ lie on a regular grid with possibly non-uniform mesh, of dimension $M_1 \times M_2 \times \ldots \times M_d = M$:

$$\left\{(z_{1,j_1}, z_{2,j_2}, \ldots, z_{d,j_d}) \in \mathbb{R}^d,\ j_k \in \{1, 2, \ldots, M_k\},\ k \in \{1, 2, \ldots, d\}\right\}$$

Figure 4 on page 18 provides two examples of rectilinear evaluation grids in the bivariate case.

Condition 2. [Kernel support] We allow the bandwidths to vary with the evaluation points (balloon estimators, see subsection 3.2) but require them to follow the shape of the evaluation grid. In other words, each evaluation point $z_j = (z_{1,j_1}, z_{2,j_2}, \ldots, z_{d,j_d})$ is associated with its own bandwidth $h_j = (h_{1,j_1}, h_{2,j_2}, \ldots, h_{d,j_d})$. For kernels with finite support (first eight kernels in Table 1), this means that the kernel support must be a hyperrectangle, i.e. the box

$$\begin{aligned}&\prod_{k=1}^d [z_{k,j_k} - h_{k,j_k}, z_{k,j_k} + h_{k,j_k}] \\ &:= \left\{(u_1, u_2, \ldots, u_d) \in \mathbb{R}^d \,|u_k \in [z_{k,j_k} - h_{k,j_k}, z_{k,j_k} + h_{k,j_k}], k = 1, 2, \ldots, d\right\}\end{aligned}$$

where $j_k \in \{1, 2, \ldots, M_k\}$, $k \in \{1, 2, \ldots d\}$.

The reason for these two conditions will become clear after the description of the multivariate sweeping algorithm for multivariate sum updating. In the rest of this section, we assume these two conditions are satisfied. The next subsection discusses the choice of multivariate kernel, and show that two simple types of multivariate kernels satisfy Condition 2: product kernels (equation (10)) and average kernels (equation (11)).

2.3.3. Multivariate kernel

To extend the definitions of the smoothing kernels (1), (2) and (3) to the multivariate case, one needs kernel functions defined in a multivariate setting. There exists different ways to extend a univariate kernel to the multivariate case, see Härdle and Müller (2000) for example. As an illustration, Figure 1 displays three different ways to extend the Epanechnikov kernel $K_1(u) = \frac{3}{4}(1-u^2)$ to the multivariate (bivariate) case.

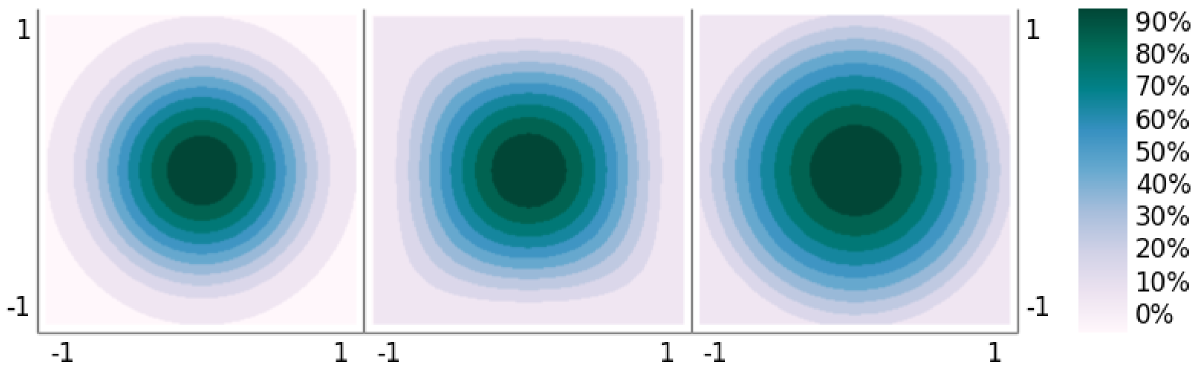

Figure 1: Bivariate parabolic kernels

The left-side kernel in Figure 1 corresponds to the *spherical* or *radially symmetric* kernel:

$$K_d^S(u_1,\dots,u_d) = \frac{\Gamma\left(2+\frac{d}{2}\right)}{\pi^{\frac{d}{2}}}\left(1-\|u\|^2\right)\mathbb{1}\{\|u\|\le 1\} \tag{9}$$

for which the norm of the vector u is used as an input in the univariate kernel (with a proper normalization constant, see Fukunaga and Hostetler (1975)). This multivariate kernel is the most efficient in terms of asymptotic mean integrated squared error (see Wand and Jones (1995) for example). Unfortunately, this kernel is not compatible with fast sum updating, as its support is a hypersphere, while Condition 2 requires a hyperrectangle support. The middle kernel in Figure 1 corresponds to the *multiplicative* or *product* kernel:

$$K_d^P(u_1,\dots,u_d) = \prod_{k=1}^{d} K_1(u_k) = \left(\frac{3}{4}\right)^d \prod_{k=1}^{d}\left\{\left(1-u_k^2\right)\mathbb{1}\{|u_k|\le 1\}\right\} \tag{10}$$

obtained by multiplying univariate kernels. Its support is a hyperrectangle. Finally, the right-side kernel in Figure 1 corresponds to the *additive* or *arithmetic average* kernel:

$$K_d^A(u_1,\dots,u_d) = \frac{1}{d2^{d-1}}\sum_{k=1}^{d} K_1(u_k)\prod_{\substack{k_0=1\\k_0\neq k}}^{d}\mathbb{1}\{|u_{k_0}|<1\} = \frac{3}{d2^{d+1}}\sum_{k=1}^{d}\left(1-u_k^2\right)\prod_{k_0=1}^{d}\mathbb{1}\{|u_{k_0}|<1\} \tag{11}$$

which is obtained by averaging univariate kernels, and is another general way of producing multivariate kernels. The support of this kernel is also a hyperrectangle. As Condition 2 rules out the spherical kernel (9), we have to make a choice between the product kernel (10) and the average kernel (11). When it comes to choosing a kernel, the following quote from Silverman

(1982) summarizes the general consensus in the literature: *"Both theory and practice suggest that the choice of kernel is not crucial to the statistical performance of the method and therefore it is quite reasonable to choose a kernel for computational efficiency"*. In our context, this observation means that the average kernel (11) is to be preferred over the product kernel (10) for its greater computational efficiency. Indeed, while average kernels are not as efficient[1] as product kernels (see Table 2) they contain much fewer sums to track down for the fast sum updating algorithm (after expanding the squared terms $(x_{k,i}-z_{k,j})^2/h_k^2$, the sum (8) is composed of 3^d different sums over $i=1,\dots,N$ for the product kernel (10), compared to only $2d+1$ sums for the average kernel (11)). In the end, to achieve the same accuracy, the average kernel (11) is vastly faster than the product kernel (10) when using the fast sum updating approach (around 80% faster for bivariate problems, more than 18 times faster for five-dimensional problems, see Table 2). For this reason, we henceforth use the average multivariate kernel (11) in the rest of the paper.

dimension	2D	3D	4D	5D
K^P efficiency	98.2%	95.3%	91.6%	87.4%
K^A efficiency	96.5%	88.9%	80.4%	71.8%
K^P number of sums	9	27	81	243
K^A number of sums	5	7	9	11
speedup factor of K^A over K^P	1.8	3.6	7.9	18.2

Table 2: product kernel K^P vs. average kernel K^A

2.3.4. Kernel expansion

Using the multivariate kernel (11), one can expand the sum (8) as follows:

$$\begin{aligned}
\mathbf{S}_j := \mathbf{S}_{k_1,k_2,j}^{p_1,p_2,q} &= \frac{1}{N\prod_{k=1}^d h_k}\sum_{i=1}^N K_d\left(\frac{x_{1,i}-z_{1,j}}{h_1},\frac{x_{2,i}-z_{2,j}}{h_2},\dots,\frac{x_{d,i}-z_{d,j}}{h_d}\right)x_{k_1,i}^{p_1}x_{k_2,i}^{p_2}y_i^q \\
&= \frac{3}{d2^{d+1}N\prod_{k=1}^d h_k}\sum_{i=1}^N\sum_{k=1}^d\left(1-\frac{(x_{k,i}-z_{k,j})^2}{h_k^2}\right)x_{k_1,i}^{p_1}x_{k_2,i}^{p_2}y_i^q\prod_{k_0=1}^d \mathbb{1}\{|x_{k_0,i}-z_{k_0,j}|\le 1\} \\
&= \frac{3}{d2^{d+1}N\prod_{k=1}^d h_k}\sum_{k=1}^d\sum_{i=1}^N\left(1-\frac{z_{k,j}^2}{h_k^2}+2\frac{z_{k,j}}{h_k^2}x_{k,i}-\frac{1}{h_k^2}x_{k,i}^2\right)x_{k_1,i}^{p_1}x_{k_2,i}^{p_2}y_i^q\prod_{k_0=1}^d \mathbb{1}\{|x_{k_0,i}-z_{k_0,j}|\le 1\} \\
&= \frac{3}{d2^{d+1}N\prod_{k=1}^d h_k}\sum_{k=1}^d\left\{\left(1-\frac{z_{k,j}^2}{h_k^2}\right)\mathcal{S}_{[k,k_1,k_2]}^{[0,p_1,p_2],q}([z_j-h_j,z_j+h_j])+\right. \\
&= \left. 2\frac{z_{k,j}}{h_k^2}\mathcal{S}_{[k,k_1,k_2]}^{[1,p_1,p_2],q}([z_j-h_j,z_j+h_j])-\frac{1}{h_k^2}\mathcal{S}_{[k,k_1,k_2]}^{[2,p_1,p_2],q}([z_j-h_j,z_j+h_j])\right\}
\end{aligned} \tag{12}$$

[1]The efficiency $\mathrm{eff}(K)$ of a kernel K is defined as the ratio $R(K^S)\mu_2^{d/2}(K^S)/(R(K)\mu_2^{d/2}(K))$ where $R(K):=\int\cdots\int K^2(u_1,\dots,u_d)du_1\dots du_d$, $\mu_2(K):=\int\cdots\int u_1^2K(u_1,\dots,u_d)du_1\dots du_d$ and K^S is the spherical kernel (9), see Wand and Jones (1995). The speedup of K^A over K^P to achieve the same accuracy (Table 2), is defined as $3^d\mathrm{eff}(K^P)/((2d+1)\mathrm{eff}(K^A))=(18/5)^d(3d/(5d-2))^{d/2}5d/((2d+1)(5d+1))$.

where for any hyperrectangle $[\mathbf{L}, \mathbf{R}] := [L_1, R_1] \times [L_2, R_2] \times \ldots \times [L_d, R_d] \subseteq \mathbb{R}^d$:

$$\mathcal{S}^{\text{idx}}([\mathbf{L}, \mathbf{R}]) := \mathcal{S}_{\mathbf{k}}^{\mathbf{p},q}([\mathbf{L}, \mathbf{R}]) := \sum_{i=1}^{N} \left(\prod_{l=1}^{3} (x_{k_l,i})^{p_l} \right) y_i^q \prod_{k_0=1}^{d} \mathbb{1}\{L_{k_0} \leq x_{k_0,i} \leq R_{k_0}\} \tag{13}$$

for powers $\mathbf{p} := (p_1, p_2, p_3) \in \mathbb{N}^3$, $q \in \mathbb{N}$ and indices $\mathbf{k} := (k_1, k_2, k_3) \in \{1, 2, \ldots, d\}^3$, and where $[z_j - h_j, z_j + h_j] := [z_{1,j} - h_{1,j}, z_{1,j} + h_{1,j}] \times \ldots \times [z_{d,j} - h_{d,j}, z_{d,j} + h_{d,j}]$. To simplify notations, we make use of the multi-index idx $:= (\mathbf{p}, q, \mathbf{k})$.

To sum up what has been obtained so far, computing multivariate kernel smoothers (kernel density estimation, kernel regression, locally linear regression) boils down to computing sums of the type (13) on hyperrectangles of the type $[z_j - h_j, z_j + h_j]$ for every evaluation point $j \in \{1, 2, \ldots, M\}$. In the univariate case, these sums could be computed efficiently by sorting the input points x_i, $i \in \{1, 2, \ldots, N\}$ and updating the sums from one evaluation point to the next (equation (7)). Our goal is now to set up a similar efficient fast sum updating algorithm for the multivariate sums (13). To do so, we first partition the input data into a multivariate rectilinear grid (subsection 2.3.5), by taking advantage of the fact that the evaluation grid is rectilinear (Condition 1) and that the support of the kernels has a hyperrectangle shape (Condition 2). Then, we set up a fast sweeping algorithm using the sums on each hyperrectangle of the partition as the unit blocks to be added and removed (subsection 2.3.6), unlike the univariate case where the input points themselves were being added and removed iteratively. Finally, the computational speed of this new algorithm is discussed in subsection 2.4.

2.3.5. Data partition

The first stage of the multivariate fast sum updating algorithm is to partition the sample of input points into boxes. To do so, define the sorted lists

$$\tilde{\mathcal{G}}_k = \{\tilde{g}_{k,1}, \tilde{g}_{k,2}, \ldots, \tilde{g}_{k,2M_k}\} := \text{sort}\Big(\{z_{k,j_k} - h_{k,j_k}\}_{j_k \in \{1,2,\ldots,M_k\}} \bigcup \{z_{k,j_k} + h_{k,j_k}\}_{j_k \in \{1,2,\ldots,M_k\}}\Big)$$

in each dimension $k \in \{1, 2, \ldots, d\}$, and define the partition intervals $\tilde{I}_{k,l} := [\tilde{g}_{k,l}, \tilde{g}_{k,l+1}]$ for $l \in \{1, 2, \ldots, 2M_k - 1\}$. The second row of Figure 2 illustrates this partition on a set of 4 points, where for simplicity the evaluation points are the same as the input points. By definition of $\tilde{\mathcal{G}}_k$, all the bandwidths edges $z_{k,j_k} - h_{k,j_k}$ and $z_{k,j_k} + h_{k,j_k}$, $j_k \in \{1, 2, \ldots, M_k\}$, belong to $\tilde{\mathcal{G}}_k$. Therefore, there exists some indices $\tilde{L}_{k,j_k}$ and $\tilde{R}_{k,j_k}$ such that

$$[z_{k,j_k} - h_{k,j_k}, z_{k,j_k} + h_{k,j_k}] = [\tilde{g}_{k,\tilde{L}_{k,j_k}}, \tilde{g}_{k,\tilde{R}_{k,j_k}+1}] = \bigcup_{l_k \in \{\tilde{L}_{k,j_k}, \ldots, \tilde{R}_{k,j_k}\}} \tilde{I}_{k,l_k}.$$

From there, for any evaluation point $z_j = (z_{1,j_1}, z_{2,j_2}, \ldots, z_{d,j_d}) \in \mathbb{R}^d$, the box $[z_j - h_j, z_j + h_j] \subset \mathbb{R}^d$ can be decomposed into a union of smaller boxes:

$$\begin{aligned}
[z_j - h_j, z_j + h_j] &= [z_{1,j_1} - h_{1,j_1}, z_{1,j_1} + h_{1,j_1}] \times \ldots \times [z_{d,j_d} - h_{d,j_d}, z_{d,j_d} + h_{d,j_d}] \\
&= \left[\tilde{g}_{1,\tilde{L}_{1,j_1}}, \tilde{g}_{1,\tilde{R}_{1,j_1}+1}\right] \times \ldots \times \left[\tilde{g}_{d,\tilde{L}_{d,j_d}}, \tilde{g}_{d,\tilde{R}_{d,j_d}+1}\right] \\
&= \bigcup_{(l_1,\ldots,l_d) \in \{\tilde{L}_{1,j_1},\ldots,\tilde{R}_{1,j_1}\} \times \ldots \times \{\tilde{L}_{d,j_d},\ldots,\tilde{R}_{d,j_d}\}} \tilde{I}_{1,l_1} \times \ldots \times \tilde{I}_{d,l_d}
\end{aligned} \tag{14}$$

In other words, the set of boxes $\tilde{I}_{1,l_1} \times \tilde{I}_{2,l_2} \times \ldots \times \tilde{I}_{d,l_d}$ s.t. $l_k \in \{\tilde{L}_{k,j_k}, \tilde{L}_{k,j_k}+1, \ldots, \tilde{R}_{k,j_k}\}$ in each dimension $k \in \{1, 2, \ldots, d\}$ forms a partition of the box $[z_j - h_j, z_j + h_j]$. Consequently, the sum (13) evaluated on the box $[z_j - h_j, z_j + h_j]$ can be decomposed as follows:

$$\mathcal{S}^{\text{idx}}([z_j - h_j, z_j + h_j]) = \sum_{(l_1,\ldots,l_d)\in\{\tilde{L}_{1,j_1},\ldots,\tilde{R}_{1,j_1}\}\times\ldots\times\{\tilde{L}_{d,j_d},\ldots,\tilde{R}_{d,j_d}\}} \mathcal{S}^{\text{idx}}\left(\tilde{I}_{1,l_1} \times \ldots \times \tilde{I}_{d,l_d}\right) \tag{15}$$

where we assume without loss of generality that the bandwidth grid $h_j = (h_{1,j_1}, h_{2,j_2}, \ldots, h_{d,j_d})$, $j_k \in \{1, 2, \ldots, M_k\}$, $k \in \{1, 2, \ldots d\}$ is such that the list $\tilde{\mathcal{G}}_k$ does not contain any input $x_{k,i}$, $i \in \{1, 2, \ldots, N\}$ (as such boundary points would be counted twice in the right-hand side of (15)). This simple condition is easy to satisfy, as shown by the adaptive bandwidth example provided in subsection 3.2.

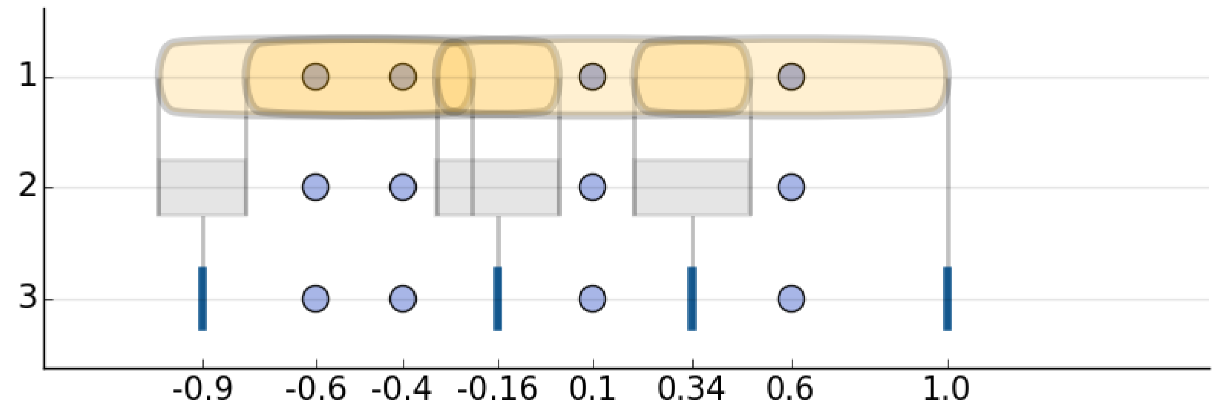

Figure 2: From bandwidths to partition (1D)

The sum decomposition (15) is the cornerstone of the fast multivariate sum updating algorithm, but before going further, one can simplify the partitions $\tilde{\mathcal{G}}_k$, $k \in \{1, 2, \ldots, d\}$ while maintaining a sum decomposition of the type (15). Indeed, in general some intervals $\tilde{I}_{k,l}$ might be empty (i.e. they might not contain any input point $x_{k,i}$, cf. the grey intervals on the second row of Figure 2). To avoid keeping track of sums $\mathcal{S}^{\text{idx}}$ on boxes known to be empty, one can trim the partitions $\tilde{\mathcal{G}}_k$ by replacing each succession of empty intervals by one new partition threshold. For example, if $\tilde{I}_{k,l} = [\tilde{g}_{k,l}, \tilde{g}_{k,l+1}]$ is empty, one can remove the two points $\tilde{g}_{k,l}$ and $\tilde{g}_{k,l+1}$ and replace them by, for example, $(\tilde{g}_{k,l} + \tilde{g}_{k,l+1})/2$ (cf. the final partition on the third row of Figure 2). Denote by $\mathcal{G}_k = \{g_{k,1}, g_{k,2}, \ldots, g_{k,m_k}\}$ the sorted simplified list, where $2 \leq m_k \leq 2M_k$, $k \in \{1, 2, \ldots, d\}$, and $m := \prod_{k=1}^{d} m_k \leq 2^d M$. Define the new partition intervals $I_{k,l} := [g_{k,l}, g_{k,l+1}]$, $l \in \{1, 2, \ldots, m_k - 1\}$. Because the trimming from $\tilde{\mathcal{G}}_k$ to $\mathcal{G}_k$ only affects the empty intervals, the following still holds:

Lemma 2.1. *For any evaluation point $z_j = (z_{1,j_1}, z_{2,j_2}, \ldots, z_{d,j_d}) \in \mathbb{R}^d$, $j_k \in \{1, 2, \ldots, M_k\}$, $k \in \{1, 2, \ldots d\}$, there exists indices $(L_{1,j_1}, L_{2,j_2}, \ldots, L_{d,j_d})$ and $(R_{1,j_1}, R_{2,j_2}, \ldots, R_{d,j_d})$, where $L_{k,j_k} \in \{1, 2, \ldots, m_k - 1\}$ and $R_{k,j_k} \in \{1, 2, \ldots, m_k - 1\}$ with $L_{k,j_k} \leq R_{k,j_k}$, $k \in \{1, 2, \ldots d\}$, such that*

$$\mathcal{S}^{\text{idx}}([z_j - h_j, z_j + h_j]) = \sum_{(l_1,\ldots,l_d)\in\{L_{1,j_1},\ldots,R_{1,j_1}\}\times\ldots\times\{L_{d,j_d},\ldots,R_{d,j_d}\}} \mathcal{S}^{\text{idx}}(I_{1,l_1} \times \ldots \times I_{d,l_d}) \tag{16}$$

For later use, we introduce the compact notation $\mathcal{S}^{\text{idx}}_{l_1,l_2,\ldots,l_d} := \mathcal{S}^{\text{idx}}(I_{1,l_1} \times \ldots \times I_{d,l_d})$. Recalling equation (13), the sum $\mathcal{S}^{\text{idx}}_{l_1,l_2,\ldots,l_d}$ corresponds to the sum of the polynomials $(\prod_{l=1}^{3}(x_{k_l,i})^{p_l})y_i^q$ over all the data points within the box $I_{1,l_1} \times \ldots \times I_{d,l_d}$.

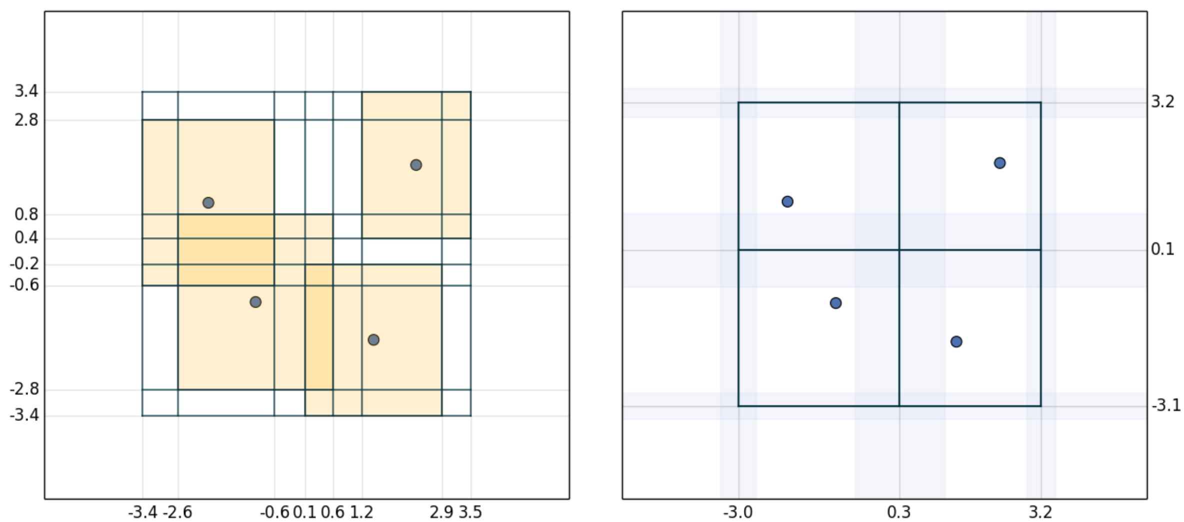

Figure 3: From bandwidths to partition (2D)

To complement the illustration of univariate partition given by Figure 2, Figure 3 provides a bivariate partition example. There are four points, each at the center of their respective rectangular kernel (in orange). On the left-hand side, the bandwidths boundaries are used to produce the partitions $\tilde{\mathcal{G}}_k$ in each dimension. One can see that most of the resulting rectangles are empty. On the right-hand side, the empty rectangles are removed/merged, resulting in the trimmed partitions $\mathcal{G}_k$ in each dimension. Remark that this is a simple example for which every final rectangle only contains one point.

2.3.6. Fast multivariate sweeping algorithm

So far, we have shown that computing multivariate kernel smoothers is based on the computation of the kernel sums (8), which can be decomposed into sums of the type (13), which can themselves be decomposed into the smaller sums (16) by decomposing every kernel support of every evaluation point onto the box partition described in the previous subsection 2.3.5. The final task is to define an efficient algorithm to traverse all the hyperrectangle unions $\bigcup_{(l_1,\ldots,l_d)\in\{L_{1,j_1},\ldots,R_{1,j_1}\}\times\ldots\times\{L_{d,j_d},\ldots,R_{d,j_d}\}} I_{1,l_1} \times \ldots \times I_{d,l_d}$, so as to compute the right-hand side sums in equation (16) (Lemma 2.1) in an efficient fast sum updating way similar to the univariate updating (7). We precompute all the sums $\mathcal{S}^{\text{idx}}_{l_1,l_2,\ldots,l_d}$ with idx $= (\mathbf{p}, q, \mathbf{k}) \in \{0,1,2\} \times \{0,1\}^3 \times \{1,2,\ldots,d\}^3$, and use them as input material for fast multivariate sum updating.

We start with the bivariate case, summarized in Algorithm 2, with the help of Figures 12 and 13. We first provide an algorithm to compute the sums $\mathcal{T}^{\text{idx}}_{1,l_2} := \sum_{l_1=L_{1,j_1}}^{R_{1,j_1}} \mathcal{S}^{\text{idx}}_{l_1,l_2}$, for every $l_2 \in \{1,2,\ldots,m_2-1\}$ and every index interval $[L_{1,j_1}, R_{1,j_1}]$, $j_1 \in \{1,2,\ldots,M_1\}$. Starting with

$j_1 = 1$, we first compute $\mathcal{T}_{1,l_2}^{\text{idx}} = \sum_{l_1=L_{1,1}}^{R_{1,1}} \mathcal{S}_{l_1,l_2}^{\text{idx}}$ for every $l_2 \in \{1, 2, \ldots, m_2 - 1\}$. Then we iteratively increment j_1 from $j_1 = 1$ to $j_1 = M_1$. After each incrementation of j_1, we update $\mathcal{T}_{1,l_2}^{\text{idx}}$ by fast sum updating

$$\sum_{l_1=L_{1,j_1}}^{R_{1,j_1}} \mathcal{S}_{l_1,l_2}^{\text{idx}} = \sum_{l_1=L_{1,j_1-1}}^{R_{1,j_1-1}} \mathcal{S}_{l_1,l_2}^{\text{idx}} + \sum_{l_1=R_{1,j_1-1}+1}^{R_{1,j_1}} \mathcal{S}_{l_1,l_2}^{\text{idx}} - \sum_{l_1=L_{1,j_1-1}}^{L_{1,j_1}-1} \mathcal{S}_{l_1,l_2}^{\text{idx}} \tag{17}$$

The second stage is to perform a fast sum updating in the second dimension, with the sums $\mathcal{T}_{1,l_2}^{\text{idx}} = \sum_{l_1=L_{1,j_1}}^{R_{1,j_1}} \mathcal{S}_{l_1,l_2}^{\text{idx}}$ as input material. Our goal is to compute the sums $\mathcal{T}_2^{\text{idx}} := \sum_{l_2=L_{2,j_2}}^{R_{2,j_2}} \mathcal{T}_{1,l_2}^{\text{idx}}$ for every index interval $[L_{2,j_2}, R_{2,j_2}]$, $j_2 \in \{1, 2, \ldots, M_2\}$. In a similar manner, we start from $j_2 = 1$ with the initial sum $\mathcal{T}_2^{\text{idx}} = \sum_{l_2=L_{2,1}}^{R_{2,1}} \mathcal{T}_{1,l_2}^{\text{idx}}$. We then increment j_2 from $j_2 = 1$ to $j_2 = M_2$ iteratively. After each incrementation of j_2, we update $\mathcal{T}_2^{\text{idx}}$ by fast sum updating:

$$\sum_{l_2=L_{2,j_2}}^{R_{2,j_2}} \mathcal{T}_{1,l_2}^{\text{idx}} = \sum_{l_2=L_{2,j_2-1}}^{R_{2,j_2-1}} \mathcal{T}_{1,l_2}^{\text{idx}} + \sum_{l_2=R_{2,j_2-1}+1}^{R_{2,j_2}} \mathcal{T}_{1,l_2}^{\text{idx}} - \sum_{l_2=L_{2,j_2-1}}^{L_{2,j_2}-1} \mathcal{T}_{1,l_2}^{\text{idx}} \tag{18}$$

Using Lemma 2.1 (equation (16)), the resulting sum $\sum_{l_2=L_{2,j_2}}^{R_{2,j_2}} \mathcal{T}_{1,l_2}^{\text{idx}} = \sum_{l_1=L_{1,j_1}}^{R_{1,j_1}} \sum_{l_2=L_{2,j_2}}^{R_{2,j_2}} \mathcal{S}_{l_1,l_2}^{\text{idx}}$ is equal to $\mathcal{S}^{\text{idx}}([z_j - h_j, z_j + h_j])$, which can be used to compute the kernel sums $\mathbf{S}_j$ using equation (12), from which the bivariate kernel smoothers (kernel density estimator, kernel regression, locally linear regression) can be computed.

This ends the description of the fast sum updating algorithm in the bivariate case. A graphical description of it is available in Appendix D. The reason for enforcing Condition 1 and Condition 2 is now clear: they pave the way for the box partition described in subsection 2.3.5, from which the iterative fast sum updating, one dimension at a time, displayed on Figures 12 and 13, can cover all the multivariate bandwidths of all the evaluation points on the evaluation grid.

Finally, the general multivariate case is a straightforward extension of the bivariate case, and is summarized in Algorithm 3.

Algorithm 2: Fast bivariate kernel smoothing

Input: precomputed sums $\mathcal{S}^{\text{idx}}_{l_1,l_2}$

$\text{iL}_1 = 1$
$\text{iR}_1 = 1$
$\mathcal{T}^{\text{idx}}_{1,l_2} = 0$
for $j_1 = 1, ..., M_1$ **do**
  while ($\text{iR}_1 < m_1$) *and* ($\text{iR}_1 \leq R_{1,j_1}$) **do**
    $\mathcal{T}^{\text{idx}}_{1,l_2} = \mathcal{T}^{\text{idx}}_{1,l_2} + \mathcal{S}^{\text{idx}}_{\text{iR}_1,l_2}, \forall l_2 \in \{1, 2, \ldots, m_2 - 1\}$
    $\text{iR}_1 = \text{iR}_1 + 1$
  end
  while ($\text{iL}_1 < m_1$) *and* ($\text{iL}_1 < L_{1,j_1}$) **do**
    $\mathcal{T}^{\text{idx}}_{1,l_2} = \mathcal{T}^{\text{idx}}_{1,l_2} - \mathcal{S}^{\text{idx}}_{\text{iL}_1,l_2}, \forall l_2 \in \{1, 2, \ldots, m_2 - 1\}$
    $\text{iL}_1 = \text{iL}_1 + 1$
  end
  ▷ Here $\mathcal{T}^{\text{idx}}_{1,l_2} = \sum_{l_1=L_{1,j_1}}^{R_{1,j_1}} \mathcal{S}^{\text{idx}}_{l_1,l_2}$, $\forall l_2 \in \{1, 2, \ldots, m_2 - 1\}$
  $\text{iL}_2 = 1$
  $\text{iR}_2 = 1$
  $\mathcal{T}^{\text{idx}}_2 = 0$
  for $j_2 = 1, ..., M_2$ **do**
    while ($\text{iR}_2 < m_2$) *and* ($\text{iR}_2 \leq R_{2,j_2}$) **do**
      $\mathcal{T}^{\text{idx}}_2 = \mathcal{T}^{\text{idx}}_2 + \mathcal{T}^{\text{idx}}_{1,\text{iR}_2}$
      $\text{iR}_2 = \text{iR}_2 + 1$
    end
    while ($\text{iL}_2 < m_2$) *and* ($\text{iL}_2 < L_{2,j_2}$) **do**
      $\mathcal{T}^{\text{idx}}_2 = \mathcal{T}^{\text{idx}}_2 - \mathcal{T}^{\text{idx}}_{1,\text{iL}_2}$
      $\text{iL}_2 = \text{iL}_2 + 1$
    end
    ▷ Here $\mathcal{T}^{\text{idx}}_2 = \sum_{l_1=L_{1,j_1}}^{R_{1,j_1}} \sum_{l_2=L_{2,j_2}}^{R_{2,j_2}} \mathcal{S}^{\text{idx}}_{l_1,l_2}$
    ▷ $= \mathcal{S}^{\mathbf{p},q}_{\mathbf{k}}([z_j - h_j, z_j + h_j])$ from equation (16)
    Compute $\mathbf{S}_j$ using $\mathcal{T}^{\text{idx}}_2$ and equation (12)
    Compute multivariate kernel smoothers using $\mathbf{S}_j$
  end
end

Output: Bivariate kernel smoothers

Algorithm 3: Fast multivariate kernel smoothing

Input: precomputed sums $\mathcal{S}^{\text{idx}}_{l_1,l_2,\ldots,l_d}$

```
iL_1 = 1, iR_1 = 1, T^idx_{1,l_2,l_3,...,l_d} = 0
for j_1 = 1, ..., M_1 do
    while ( iR_1 < m_1 ) and ( iR_1 ≤ R_{1,j_1} ) do
        T^idx_{1,l_2,l_3,...,l_d} = T^idx_{1,l_2,l_3,...,l_d} + S^idx_{iR_1,l_2,l_3,...,l_d}, ∀l_k∈{1,2,...,m_k−1}, k∈{2,3,...,d}
        iR_1 = iR_1 + 1
    end
    while ( iL_1 < m_1 ) and ( iL_1 < L_{1,j_1} ) do
        T^idx_{1,l_2,l_3,...,l_d} = T^idx_{1,l_2,l_3,...,l_d} − S^idx_{iL_1,l_2,l_3,...,l_d}, ∀l_k∈{1,2,...,m_k−1}, k∈{2,3,...,d}
        iL_1 = iL_1 + 1
    end
    ▷ Here T^idx_{1,l_2,l_3,...,l_d} = Σ_{l_1=L_{1,j_1}}^{R_{1,j_1}} S^idx_{l_1,l_2,...,l_d}, ∀l_k∈{1,2,...,m_k−1}, k∈{2,3,...,d}
    iL_2 = 1, iR_2 = 1, T^idx_{2,l_3,...,l_d} = 0
    for j_2 = 1, ..., M_2 do
        while ( iR_2 < m_2 ) and ( iR_2 ≤ R_{2,j_2} ) do
            T^idx_{2,l_3,...,l_d} = T^idx_{2,l_3,...,l_d} + T^idx_{1,iR_2,l_3,...,l_d}, ∀l_k∈{1,2,...,m_k−1}, k∈{3,...,d}
            iR_2 = iR_2 + 1
        end
        while ( iL_2 < m_2 ) and ( iL_2 < L_{2,j_2} ) do
            T^idx_{2,l_3,...,l_d} = T^idx_{2,l_3,...,l_d} − T^idx_{1,iL_2,l_3,...,l_d}, ∀l_k∈{1,2,...,m_k−1}, k∈{3,...,d}
            iL_2 = iL_2 + 1
        end
        ▷ T^idx_{2,l_3,...,l_d} = Σ_{l_1=L_{1,j_1}}^{R_{1,j_1}} Σ_{l_2=L_{2,j_2}}^{R_{2,j_2}} S^idx_{l_1,l_2,...,l_d}, ∀l_k∈{1,...,m_k−1}, k∈{3,...d}
        ⋮
        iL_d = 1, iR_d = 1, T_d = 0
        for j_d = 1, ..., M_d do
            while ( iR_d < m_d ) and ( iR_d ≤ R_{d,j_d} ) do
                T^idx_d = T^idx_d + T^idx_{d−1,iR_d}
                iR_d = iR_d + 1
            end
            while ( iL_d < m_d ) and ( iL_d < L_{d,j_d} ) do
                T^idx_d = T^idx_d − T^idx_{d−1,iL_d}
                iL_d = iL_d + 1
            end
            ▷ Here T^idx_d = Σ_{l_1=L_{1,j_1}}^{R_{1,j_1}} Σ_{l_2=L_{2,j_2}}^{R_{2,j_2}} ··· Σ_{l_d=L_{d,j_d}}^{R_{d,j_d}} S^idx_{l_1,l_2,...,l_d}
            ▷ = S^{p,q}_k([z_j − h_j, z_j + h_j]) from equation (16)
            Compute S_j using T^idx_d and equation (12)
            Compute multivariate kernel smoothers using S_j
        end
    end
end
```

Output: Multivariate kernel smoothers

2.4. Complexity

2.4.1. Computational complexity

One can verify that the number of operations in the multivariate fast sum updating algorithm 3 is proportional to the number of evaluation points $M = M_1 \times M_2 \times \ldots \times M_d$. Indeed, recall from subsection 2.3.5 that in each dimension $k \in \{1, 2, \ldots, d\}$, $m_k - 1$ is the number of intervals in the k-th dimension of the data partition, with $2 \leq m_k \leq 2M_k$. The first two *while* loops over iR_1 and iL_1 in Algorithm 3 generate $2(m_1 - 1)$ updates of the sums $\mathcal{T}^{\mathrm{idx}}_{1,l_2,l_3,\ldots,l_d}$ of size $(m_2 - 1) \times \ldots \times (m_d - 1)$, for a total of $\mathcal{O}(M)$ operations. Then, the two subsequent *while* loops over iR_2 and iL_2 generate $M_1 \times 2(m_2 - 1)$ updates of the sums $\mathcal{T}^{\mathrm{idx}}_{2,l_3,\ldots,l_d}$ of size $(m_3 - 1) \times \ldots \times (m_d - 1)$, for a total of $\mathcal{O}(M)$ operations. The final *while* loops over iR_d and iL_d generate $M_1 \times \ldots \times M_{d-1} \times 2(m_d - 1) = \mathcal{O}(M)$ updates of the sum $\mathcal{T}^{\mathrm{idx}}_d$ of size 1. The computational complexity of Algorithm 3 is therefore $\mathcal{O}(M)$.

In addition to this cost, Algorithm 3 requires the construction of the partition $\mathcal{G}_k$ and of the threshold indices $L_{k,j_k} \in \{1, 2, \ldots, m_k - 1\}$ and $R_{k,j_k} \in \{1, 2, \ldots, m_k - 1\}$ (recall Lemma 2.1), which costs $\mathcal{O}(M)$ operations or $\mathcal{O}(M \log M)$ is the evaluation points are not sorted. The precomputation of the sums $\mathcal{S}^{\mathrm{idx}}_{l_1,l_2,\ldots,l_d}$ costs $\mathcal{O}(N)$ operations once the input sample $(x_{1,i}, x_{2,i}, \ldots, x_{d,i})$, $i \in \{1, 2, \ldots, N\}$ has been sorted in each dimension independently, at a cost of $\mathcal{O}(N \log N)$ operations. The total computational complexity of the multivariate fast sum updating algorithm described in this section is therefore $\mathcal{O}(M \log M + N \log N)$, which is a considerable improvement over the $\mathcal{O}(M \times N)$ complexity of the naive approach.

2.4.2. Memory complexity

The memory comsumption of Algorithm 3 stems from the simultaneous storage of the sums $\mathcal{S}^{\mathrm{idx}}_{l_1,l_2,\ldots,l_d}$, $\mathcal{T}^{\mathrm{idx}}_{1,l_2,l_3,\ldots,l_d}$, $\mathcal{T}^{\mathrm{idx}}_{2,l_3,\ldots,l_d}$, $\ldots$, $\mathcal{T}^{\mathrm{idx}}_d$ for every $l_k \in \{1, 2, \ldots, m_k - 1\}$, $k \in \{2, 3, \ldots, d\}$ and $\mathrm{idx} = (\mathbf{p}, q, \mathbf{k}) \in \{0, 1, 2\} \times \{0, 1\}^3 \times \{1, 2, \ldots, d\}^3$, resulting in a memory complexity of $\mathcal{O}(M)$.

2.4.3. Dependence in d

Finally, we look at the dependence in the dimension d of the constant in the computational and memory complexities of the algorithm. In the worst case, m_k is equal to its upper bound $2M_k$ in every dimension $k \in \{1, 2, \ldots, d\}$. In such a case, Algorithm 3 generates $\mathcal{O}(2^d M)$ operations for a single index calculation resulting in a global cost in $\mathcal{O}(d^3 2^d M)$, where d^3 comes from the dimension of the multi-index $\mathrm{idx} = (\mathbf{p}, q, \mathbf{k}) \in \{0, 1, 2\} \times \{0, 1\}^3 \times \{1, 2, \ldots, d\}^3$ as well as the fact that solving the regression system (23) costs $\mathcal{O}(d^3)$ operations for each evaluation point z_j, $j \in \{1, 2, \ldots, M\}$. In practice, the constant 2^d can be greatly reduced depending on the size of the slimmed down partition $\{\mathcal{G}_k\}_{k=1,\ldots,d}$ compared to the initial partition $\{\tilde{\mathcal{G}}_k\}_{k=1,\ldots,d}$. Similarly, the worst case memory storage needed for the sums $\mathcal{S}^{\mathrm{idx}}_{l_1,l_2,\ldots,l_d}$ and the terms $\mathcal{T}^{\mathrm{idx}}_{1,l_2,l_3,\ldots,l_d}$, $\mathcal{T}^{\mathrm{idx}}_{2,l_3,\ldots,l_d}$, $\ldots$, $\mathcal{T}^{\mathrm{idx}}_d$ is $\mathcal{O}(d^3 2^d M)$ where again the constant 2^d can be greatly reduced in practice. The sorting of the input points and evaluation points in each dimension and the precomputation of sums and indices generate altogether $\mathcal{O}(dM \log M + dN \log N)$ operations. The total computational complexity is therefore $\mathcal{O}(dM(\log M + d^2 2^d) + dN \log N)$ in the worst case, with the term 2^d possibly smaller in practice.

By contrast, the naive approach requires $\mathcal{O}(d^2 M \times (N + d))$ operations: for each $j \in \{1, 2, \ldots, M\}$, one needs $\mathcal{O}(dN)$ for computing $K_{d,h}(x_i - z_j)$ for each $i \in \{1, 2, \ldots, N\}$ (equation (11)), $\mathcal{O}(d^2 N)$

for computing all the sums in (23) and $\mathcal{O}(d^3)$ for solving the system (23). This shows that the multivariate fast sum updating is faster than the naive approach whenever $d2^d \ll N$, and still likely to be faster beyond this case as the 2^d constant only occurs in the unlikely worst case scenario for which $m_k = 2M_k$ in each dimension $k \in \{1, 2, \ldots, d\}$.

3. Evaluation grid and adaptive bandwidth

This section suggests some suitable choices of evaluation grid and adaptive bandwidth compatible with the two conditions 1 and 2, so as to ensure a wide applicability of the fast kernel smoothers described in this paper.

3.1. Shape of evaluation grid

As explained in 2.3.1, kernel smoothing estimates can generally be improved by prerotating the input dataset into a better basis. Rotating the dataset before performing kernel density estimations has been advocated in Wand (1994) and Scott and Sain (2005) for example. Condition 1 adds another motivation for rotating the dataset. Indeed, when the natural evaluation sample is not a grid, for example when the evaluation points z_1, z_2, ..., z_M are equal to the input points x_1, x_2, ..., x_N, one needs to build a suitable intermediate evaluation grid to properly cover the input sample. The left-side of Figure 4 illustrates on a bivariate example with $N = 100$ input points the potential problem of rectilinear evaluation grids when the dimensions of the input dataset are dependent: some evaluation points can be left away from the dataset. As some evaluation points are located in empty areas, the effective number of evaluation points is decreased. A rotation of the input dataset can mitigate or eliminate this problem, as shown on the right-side of Figure 4.

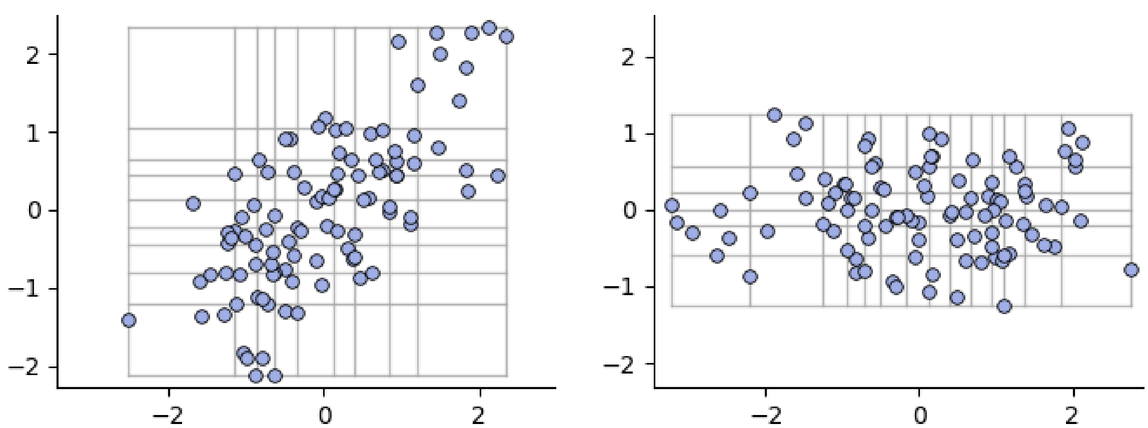

Figure 4: Evaluation grid: rotation

To construct the rotation, several techniques can be used. One possible choice is to rotate the dataset onto its principal components (as shown on Figure 4). To define the evaluation grid $\{(z_{1,j_1}, z_{2,j_2}, \ldots, z_{d,j_d}),\ j_k \in \{1, 2, \ldots, M_k\},\ k \in \{1, 2, \ldots, d\}\}$, one can first set each M_k to $M^{\frac{1}{d}}$ and define

$$z_{k,j_k} = x_{k,\mathrm{round}\left(1+(N-1)\times\frac{j_k-1}{M_k-1}\right)}$$

where round(u) is the closest integer to $u \in \mathbb{R}$ and the input set $x_1, x_2, \ldots, x_N$ is sorted in increasing order. Such a grid is illustrated on the left-side of Figure 4 (original dataset without rotation). One alternative choice for M_k is to set it proportional to the k-th singular value associated with the k-th principal component. In addition to improving the coverage of the input dataset by the evaluation grid (more evaluation points along the more variable input dimensions), this choice of M_k can reduce the dimension of the problem whenever some M_k are set to one due to a small singular value. This choice of M_k is illustrated on the right-side of Figure 4 (after the rotation of the input dataset), and is the one we use in the numerical section 4. Once the kernel density estimates have been obtained on the intermediate evaluation grid using the fast algorithm described in Section 2, one can interpolate the estimates from the grid to the evaluation points of interest by simple multilinear interpolation. Alternatively, one can interpolate by Inverse Distance Weighting (Shepherd (1968)). When the weights are chosen as kernels from Appendix A, this interpolation bears some similarity with kernel density estimation, and can benefit from the fast sum updating algorithm described in Section 2.

3.2. Fast adaptive bandwidth

The kernel smoothers (1), (2) and (3) can be defined with a fixed bandwidth h, or with an adaptive bandwidth which varies with either the input points or the evaluation points. When the input design is random as on Figure 4, some areas might be sparse while others will be dense. In such cases, the benefit of adaptive bandwidth is that one can maintain a uniform quality of density estimates by using a larger bandwidth in sparse areas and a smaller bandwidth in dense areas. There exists two main ways to define adaptive bandwidths: balloon bandwidths $h = h_j$ which vary with the evaluation point $j \in \{1, 2, \ldots, M\}$, and sample point bandwidths $h = h_i$ which vary with the input point $i \in \{1, 2, \ldots, N\}$, see Terrell and Scott (1992) or Scott and Sain (2005). While many univariate kernels in Table 1 are compatible with both balloon bandwidths and sample point bandwidths (see Appendix A), the data partition from subsection 2.3.5, which is required in the multivariate case, has been tailored for the balloon formulation (Condition 2), which is the one we adopt in this paper.

For the construction of the adaptive bandwidth, we adopt the K-nearest neighbor bandwidth suggested in Loftsgaarden and Quesenberry (1965), as it was shown in Terrell and Scott (1992) to perform well in multivariate settings. In addition, such a choice of bandwidth ensures that the bandwidth boundaries $\{z_{k,j_k} - h_{k,j_k}\}_{j_k=1,\ldots,M_k}$ and $\{z_{k,j_k} + h_{k,j_k}\}_{j_k=1,\ldots,M_k}$, $k = \{1, 2, \ldots, d\}$ remain in increasing order, which was implicitly assumed in Algorithms 2 and 3 for simplicity (one can easily adjust the loops to decrement instead of increment the grid indices $\mathrm{iL_k}$ and $\mathrm{iR_k}$ whenever the bandwidth boundaries are not in increasing order).

We now describe how to build these bandwidths in a fast $\mathcal{O}(M + N)$ from sorted datasets in the univariate case ($\mathcal{O}(M \log M + N \log N)$ if the datasets need to be sorted beforehand), and then discuss the extension to the multivariate case.

Let $x_1 \leq x_2 \leq \ldots \leq x_N$ be a sorted set of N sample points, and $z_1 \leq z_2 \leq \ldots \leq z_M$ be a sorted set of M evaluation points. Algorithm 4 describes an efficient algorithm to build M adaptive bandwidths h_j centered around the points z_j, $j = 1, \ldots, M$, such that each bandwidth $[z_j - h_j, z_j + h_j]$ contains exactly K sample points.

Algorithm 4: Fast univariate K-Nearest Neighbors bandwidth

Input:

X: sorted vector of N real points $X[1] \leq \ldots \leq X[N]$

Z: sorted vector of M evaluation points $Z[1] \leq \ldots \leq Z[M]$

K: number of points that each bandwidth should include ($1 \leq K \leq N$)

```
▷ The indices iL and iR define a subset X[iL], X[iL+1], ..., X[iR] of K points
iL = 1  ▷ Left index
iR = K  ▷ Right index
cM = (X[iL] + X[iR+1])/2  ▷ Middle cut
dmax = X[N] − X[1]  ▷ Maximum distance between 2 sample points
for i = 1, ..., M do
    while (iR+1<N) and (Z[i]>cM) do
        iL = iL+1
        iR = iR+1
        cM = 0.5 * (X[iL] + X[iR+1])
    end
    Hmin = max{ Z[i] − X[iL] , X[iR] − Z[i] }
    Hmax = min{ (Z[i] − X[iL−1]) × 𝟙{iL > 1} + dmax × 𝟙{iL = 1} ,
                (X[iR+1] − Z[i]) × 𝟙{iR < N} + dmax × 𝟙{iR = N} }
    H[i] = (Hmin+Hmax)/2
end
return H
```

Output:

H: for each point i, the interval $[Z[i] - H[i], Z[i] + H[i]]$ contains exactly K points

Define $i_L \in [1, \ldots, N-K+1]$ and $i_R = i_L + K - 1$. The subset $x_{i_L}, x_{i_L+1}, \ldots, x_{i_R}$ contains exactly K points. The idea of the algorithm is to enumerate all such possible index ranges $[i_L, i_R]$ from left ($i_L = 1$, $i_R = K$) to right ($i_L = N-K+1$, $i_R = N$), and to match each evaluation point z_j, $j \in \{1, 2, \ldots, N\}$ with its corresponding K-nearest-neighbors subsample $x_{i_L}, x_{i_L+1}, \ldots, x_{i_R}$.

Matching each index j to its corresponding $[i_L, i_R]$ range is simple. When $i_L = 1$, all the points z_j such that $z_j \leq (x_{i_L} + x_{i_R+1})/2$ are such that the subsample $x_{i_L}, x_{i_L+1}, \ldots, x_{i_R}$ corresponds to their K nearest neighbors. Indeed, any point greater than $(x_{i_L} + x_{i_R+1})/2$ is closer to x_{i_R+1} than to x_{i_L}, and therefore its K nearest neighbors are not $x_{i_L}, x_{i_L+1}, \ldots, x_{i_R}$.

Once all such z_j are matched to the current $[i_L, i_R]$ range, i_L and i_R are incremented until $(x_{i_L} + x_{i_R+1})/2$ is greater than the next evaluation point z_j to assign. The same procedure is then repeated until all the points are assigned to their K nearest neighbors.

Finally, once each point z_j is assigned to its K nearest neighbors $x_{i_L}, x_{i_L+1}, \ldots, x_{i_R}$, one still needs to choose the bandwidth h_j such that $[z_j - h_j, z_j + h_j]$ contains these K nearest neighbors. Such a bandwidth h_j exists but is not unique. We choose to set h_j to the average between the smallest possible h_j (equal to $\max\{z_j - x_{i_L}, x_{i_R} - z_j\}$) and the largest possible h_j (equal to $\min\{z_j - x_{i_L-1}, x_{iR+1} - z_j\}$ when $i_L - 1 \geq 1$ and $i_R + 1 \leq N$).

Figure 5 illustrates the resulting bandwidths on a random sample of 11 points, where the evaluation points and the sample points are set to be the same for simplicity. Each row repeats the whole sample, and shows the bandwidth centered around one of the 11 points, and containing

$k = 5$ points.

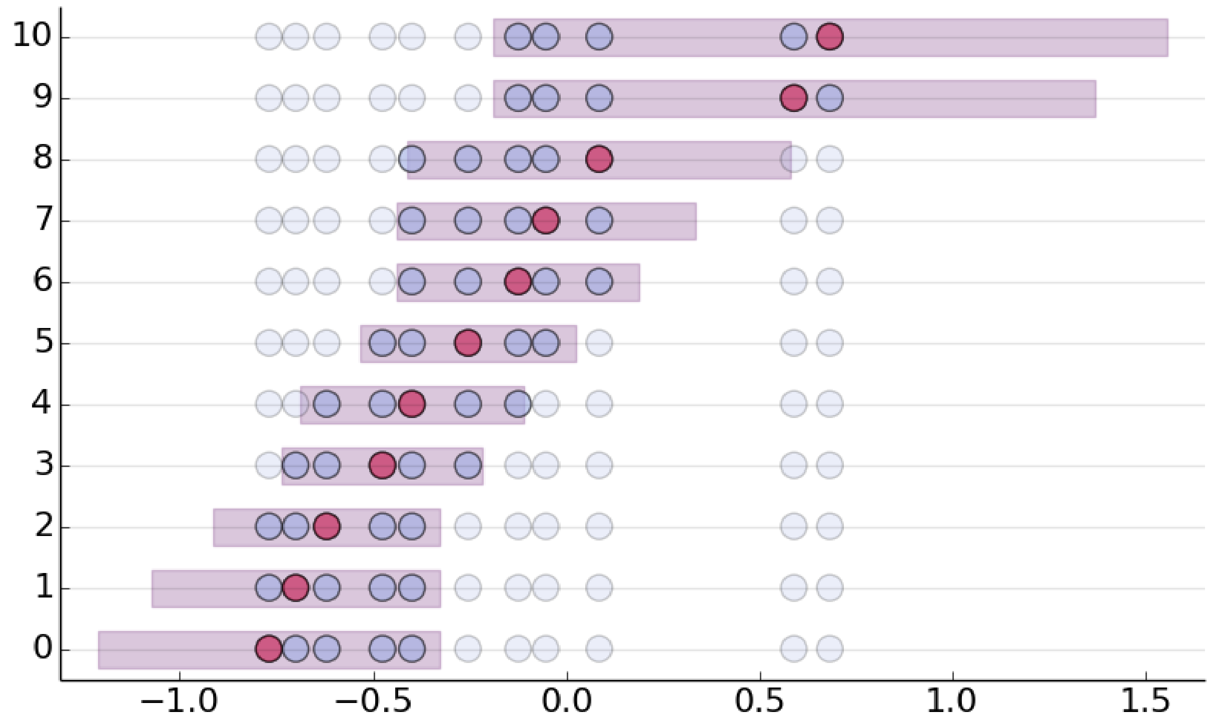

Figure 5: 1D nearest neighbour bandwidth ($N = 11$, $K = 5$)

The computational complexity of Algorithm 4 is a fast $\mathcal{O}(M + N)$ if the set of input points x_i $i \in \{1, 2, \ldots, N\}$ and the set of evaluation points z_j, $j \in \{1, 2, \ldots, M\}$ are already sorted, and $\mathcal{O}(M \log(M) + N \log(N))$ otherwise.

In the multivariate case, given Condition 2, what can be done is to compute approximate multivariate K-nearest-neighbors bandwidths by performing Algorithm 4 dimension per dimension. Let $p = K/N = p_1 \times p_2 \times \ldots \times p_d$ be the proportion of input points to include within each multivariate bandwidth. In practice, we set p_k to be inversely proportional to the k-th singular value associated with the k-th axis (projected onto $[0, 1]$ if it ends up outside this probability range) and run Algorithm 4 with $K_k = p_k \times N$ in each dimension $k \in \{1, 2, \ldots, d\}$ independently, which should ensure each multivariate bandwidth contains approximately K input points, provided the rotation onto the principal components has been performed beforehand (subsection 3.1).

4. Numerical tests

In this section, we test the fast kernel summation algorithm introduced in Section 2 and compare it to naive summation in terms of speed and accuracy. We consider a sample of N input points, choose the number of evaluation points M approximately equal to N, and build the evaluation grid and the bandwidths as described in Section 3.

From subsection 2.4, we expect a runtime proportional to $N \log(N)$. We are going to verify this result numerically. Then, we are going to compare the estimates obtained by fast kernel summation to those obtain by naive summation. As discussed in subsection 2.2, we expect small differences coming from the rounding of floats, which can be reduced or removed altogether by the use of stable summation algorithm. As a simple illustration, we measure the accuracy improvement provided by the simple Møller-Kahan algorithm (Møller (1965), Linnainmaa (1974), Ozawa (1983), see Appendix B). Beyond this simple stability improvement , one can instead use exact summation algorithms to remove any float rounding errors while maintaining the $\mathcal{O}(N\log(N))$ complexity (cf. subsection 2.2).

The input sample can be chosen arbitrarily as it does not affect the speed or accuracy of the two algorithms. We therefore simply choose to simulate N points from a d-dimensional Gaussian random variable $X \sim \mathbb{N}(0, 0.6\mathbf{1_d})$. In addition to the input sample $x_1, x_2, \ldots, x_N$, we need an output sample $y_1, y_2, \ldots, y_N$, in order to test the locally linear regression. Similarly to the input sample, the output sample can be chosen arbitrarily. We choose to define the output as

$$\begin{aligned} Y &= f(X) + W \\ f(x) &= \sum_{i=1}^{d} x_i + \exp\left(-16\left(\sum_{i=1}^{d} x_i\right)^2\right) \end{aligned}$$

where the univariate Gaussian noise $W \sim \mathbb{N}(0, 0.7)$ is independent of X.

The various tables in this section report the following values:

Fast kernel time stands for the computational time in seconds taken by the fast kernel summation algorithm;

Naive time stands for the computational time in seconds of the naive version;

Accur Worst stands for the maximum relative error of the fast sum algorithm on the whole grid. For each evaluation point, this relative error is computed as $|E_{\text{fast}} - E_{\text{naive}}|/|E_{\text{naive}}|$ where E_{fast} and E_{naive} are the estimates obtained by the fast sum updating algorithm and the naive summation algorithm, respectively;

Accur Worst Stab stands for the maximum relative error of the fast sum algorithm with Møller-Kahan stabilization on the whole grid;

Accur Aver stands for the average relative error on the grid.

Accur Aver Stab stands for the average relative error of the fast sum algorithm with stabilization on the whole grid.

We perform the tests on an Intel® Xeon® CPU E5-2680 v4 @ 2.40GHz (Broadwell)[1]. The code was written in C++ and is available in the StOpt[2] library (Gevret et al. (2018)). Subsection 4.1 focuses on kernel density estimation, while subsection 4.2 considers locally linear regression.

4.1. Fast kernel density estimation

This subsection focuses on kernel density estimation (equation (20)). We implement and compare the fast kernel summation and the naive summation algorithms for different sample sizes N. Recalling from subsection 3.2 that our adaptive bandwidths are defined by the proportion p of neighboring sample points to include in each evaluation bandwidth, we test the two proportions $p = 15\%$ and $p = 25\%$.

[1] https://ark.intel.com/products/91754/Intel-Xeon-Processor-E5-2680-v4-35M-Cache-2_40-GHz
[2] https://gitlab.com/stochastic-control/StOpt

4.1.1. Univariate case

We first consider the univariate case. Tables 3 and 4 summarize the results obtained by Algorithm 1 with the two different bandwidths. The results are very good even without stabilization, and the use of the Møller-Kahan summation algorithm improves the accuracy by two digits for the same computational cost. As expected the computational time of the fast summation algorithm is far better than the one obtained by naive summation (less than half a second versus more than three hours for 1.28 million points for example).

Nb particles	20,000	40,000	80,000	160,000	320,000	640,000	1,280,000
Fast kernel time	0.01	0.01	0.02	0.04	0.10	0.20	0.43
Naive time	2.90	12	47	190	750	3,000	12,000
Accur Worst	1.7 E-09	1.1 E-09	8.2 E-09	1.1 E-07	3.2 E-07	1.7 E-06	5.0 E-07
Accur Worst Stab	4.8 E-12	5.1 E-13	8.3 E-12	6.9 E-12	1.5 E-11	3.9 E-10	3.1 E-11
Accur Aver	1.9 E-12	1.2 E-12	1.4 E-12	9.4 E-12	1.1 E-11	6.9 E-12	1.8 E-11
Accur Aver Stab	3.8 E-15	1.8 E-15	2.0 E-15	1.9 E-15	1.9 E-15	2.5 E-15	1.9 E-15

Table 3: 1D, bandwidth 15%

Nb particles	20,000	40,000	80,000	160,000	320,000	640,000	1,280,000
Fast kernel time	0.00	0.01	0.02	0.05	0.09	0.20	0.41
Naive time	4.20	17	67	270	1,100	4,300	17,000
Accur Worst	2.1 E-10	7.2 E-11	2.8 E-10	7.8 E-09	3.6 E-08	2.9 E-07	1.3 E-07
Accur Worst Stab	4.2 E-13	6.4 E-13	1.7 E-12	3.5 E-12	1.3 E-11	3.9 E-11	3.1 E-11
Accur Aver	2.3 E-13	8.1 E-14	9.2 E-14	1.2 E-12	2.3 E-12	2.0 E-12	3.3 E-12
Accur Aver Stab	7.6 E-16	8.0 E-16	8.1 E-16	8.7 E-16	8.8 E-16	9.0 E-16	8.9 E-16

Table 4: 1D, bandwidth 25%

The runtime of the fast summation algorithm is nearly independent of the size of the bandwidth. It is not the case for the naive implementation. Indeed the larger the bandwidth, the more input points contribute to the kernel summation (1) resulting in more operations for larger bandwidths. This independence with respect to bandwidth size is another advantage of the fast sum updating approach over alternative methods such as naive summation or dual-tree methods.

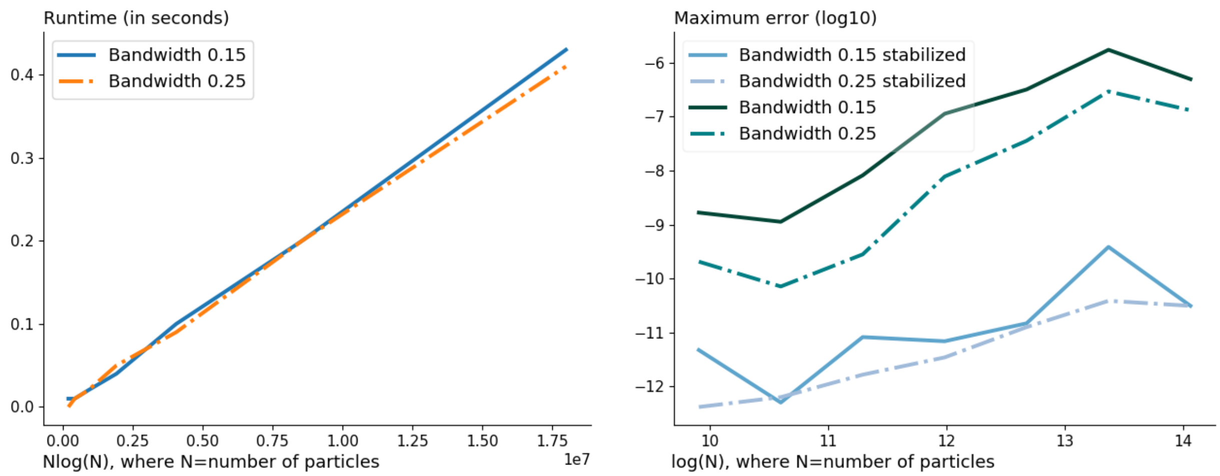

Figure 6: Speed and accuracy of fast univariate kernel summation

Figure 6 (left-hand side) clearly demonstrates that the computational time is in $N \log N$ as expected (subsection 2.4), while the right-hand side clearly demonstrates the efficiency of the stabilization. As expected, the cumulative float-rounding error slowly grows with the sample size N, but remains negligible even on the largest sample sizes.

4.1.2. Multivariate case

Tables 5 and 6 report our speed and accuracy results in the bivariate case. Once again, the fast summation algorithm is vastly faster than naive summation (less than one second versus more than seven hours for $1,28$ million points for example), and the runtime of the fast summation algorithm is independent of the size of the bandwidth. Moreover, we observe a very good accuracy (much better than the univariate case for example), even without using any summation stabilization algorithm (subsection 2.2).

Nb particles	20,000	40,000	80,000	160,000	320,000	640,000	1,280,000
Fast kernel time	0.02	0.02	0.04	0.09	0.20	0.43	0.89
Naive time	6.50	26	100	420	1,700	6,700	27,000
Accur Worst	3.2 E-12	1.9 E-12	3.0 E-10	4.5 E-10	4.0 E-11	7.2 E-08	3.5 E-09
Accur Worst Stab	4.4 E-13	1.6 E-13	3.3 E-12	1.7 E-11	4.1 E-13	1.1 E-10	3.0 E-11
Accur Aver	8.3 E-15	3.2 E-15	2.3 E-14	8.0 E-15	1.8 E-14	1.8 E-13	5.3 E-14
Accur Aver Stab	3.7 E-16	3.0 E-16	4.5 E-16	4.9 E-16	3.0 E-16	6.4 E-16	4.3 E-16

Table 5: 2D, bandwidth 15%

Nb particles	20,000	40,000	80,000	160,000	320,000	640,000	1,280,000
Fast kernel time	0.01	0.02	0.04	0.08	0.19	0.41	0.88
Naive time	8.30	33	130	540	2,100	8,700	34,000
Accur Worst	1.8 E-11	6.0 E-12	6.9 E-11	8.3 E-11	1.6 E-09	1.1 E-09	4.2 E-09
Accur Worst Stab	6.5 E-13	4.2 E-13	2.7 E-13	1.9 E-11	8.2 E-12	9.7 E-12	3.4 E-11
Accur Aver	8.5 E-15	3.8 E-15	8.7 E-15	4.6 E-15	2.7 E-14	2.1 E-14	4.8 E-14
Accur Aver Stab	3.3 E-16	3.1 E-16	2.7 E-16	6.7 E-16	4.4 E-16	2.9 E-16	5.1 E-16

Table 6: 2D, bandwidth 25%

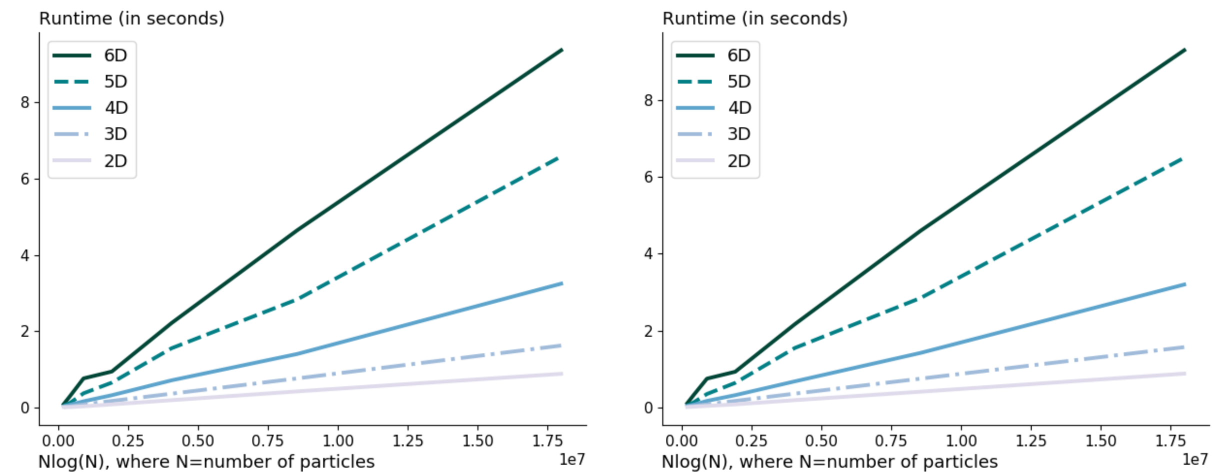

Figure 7: Runtime of fast kernel summation (left: bandwidth 15%; right: bandwidth 25%)

Figures 7 and 8 report multidimensional results up to dimension 6. Figure 7 demonstrates once again that the computational runtime is clearly in $N \log N$, while Figure 8 shows that the accuracy is very good, even without summation stabilization.

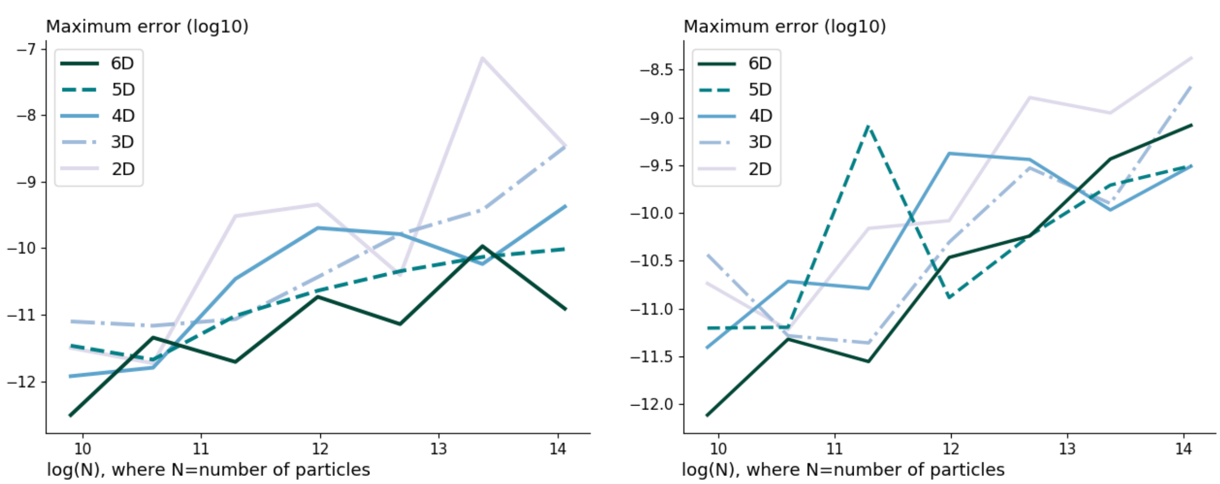

Figure 8: log10 of maximum relative error w.r.t. logN (left: bandwidth 15%; right: 25%)

4.2. Fast locally linear regression

For comprehensiveness, we now verify that our numerical observations from subsection 4.1 still hold for the harder locally linear regression problem (equations (3) and (22)).

4.2.1. Univariate case

Once again, we first consider the univariate case. Tables 7 and 8 summarize the results obtained by Algorithm 1 with the two different bandwidths. The results are very similar to the kernel density estimation case.

Figure 9 demonstrates that, as in the kernel density estimation case, the computational runtime is clearly in $N \log N$ and that the simple summation stabilization we implemented is very effective (the numerical accuracy is improved by a factor $1,500$ on average).

Nb particles	20,000	40,000	80,000	160,000	320,000	640,000	1,280,000
Fast kernel time	0.02	0.03	0.05	0.1	0.23	0.45	0.98
Naive time	4.50	18	71	280	1,100	4,500	18,000
Accur Worst	5.3 E-09	2.0 E-09	9.6 E-08	4.4 E-07	1.4 E-07	7.4 E-06	7.8 E-05
Accur Worst Stab	3.1 E-12	7.2 E-12	9.2 E-11	1.4 E-10	2.4 E-10	2.5 E-09	1.6 E-08
Accur Aver	4.4 E-12	2.1 E-12	9.1 E-12	1.4 E-11	6.1 E-12	2.9 E-11	8.5 E-11
Accur Aver Stab	5.2 E-15	5.5 E-15	6.2 E-15	5.8 E-15	6.4 E-15	9.5 E-15	2.1 E-14

Table 7: 1D results, bandwidth 15%

Nb particles	20,000	40,000	80,000	160,000	320,000	640,000	1,280,000
Fast kernel time	0.01	0.03	0.05	0.1	0.21	0.44	0.95
Naive time	6.60	26	100	420	1,700	6,700	27,000
Accur Worst	1.1 E-08	9.4 E-10	1.1 E-07	9.4 E-06	8.1 E-07	1.1 E-07	1.2 E-06
Accur Worst Stab	1.3 E-11	9.8 E-12	4.2 E-11	7.8 E-10	8.5 E-10	2.1 E-11	3.7 E-10
Accur Aver	2.3 E-12	6.6 E-13	4.3 E-12	6.9 E-11	5.8 E-12	4.6 E-12	9.4 E-12
Accur Aver Stab	2.7 E-15	2.2 E-15	2.3 E-15	8.6 E-15	4.7 E-15	1.9 E-15	2.3 E-15

Table 8: 1D results, bandwidth 25%

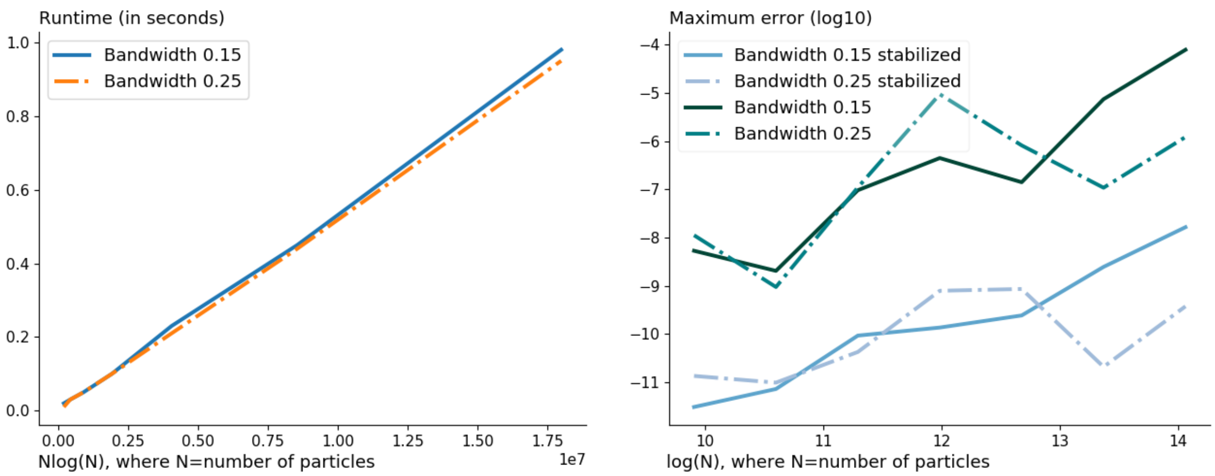

Figure 9: Speed and accuracy of fast univariate kernel summation

4.2.2. Multivariate case

Tables 9 and 10 report our speed and accuracy results in the bivariate locally linear regression case. The results are once again qualitatively very similar to the kernel density estimation case.

Nb particles	20,000	40,000	80,000	160,000	320,000	640,000	1,280,000
Fast kernel time	0.03	0.06	0.12	0.26	0.52	1.1	2.22
Naive time	9.80	40	160	630	2,500	10,000	40,000
Accur Worst	8.6 E-11	2.3 E-11	5.6 E-10	4.9 E-10	2.6 E-09	2.7 E-09	4.9 E-09
Accur Aver	5.3 E-14	1.1 E-14	5.1 E-14	2.4 E-14	7.1 E-14	9.2 E-14	1.3 E-13

Table 9: 2D results, bandwidth 15%

Nb particles	20,000	40,000	80,000	160,000	320,000	640,000	1,280,000
Fast kernel time	0.02	0.06	0.13	0.25	0.51	1.06	2.17
Naive time	14	54	220	870	3,500	14,000	56,000
Accur Worst	9.5 E-11	7.6 E-11	8.0 E-11	5.7 E-11	2.3 E-09	2.5 E-09	3.5 E-09
Accur Aver	1.7 E-14	6.3 E-15	2.4 E-14	7.3 E-15	5.9 E-14	7.2 E-14	5.0 E-14

Table 10: 2D results, bandwidth 25%

Finally, Figures 10 and 11 report multivariate locally linear regression results up to dimension 6, demonstrating once again the $N \log N$ computational complexity and the very good accuracy. Note however that compared to the kernel density estimation case, the runtime grows much more quickly with the dimension of the problem. This is due to the higher number of terms to track to perform the locally linear regressions (23) compared to one single kernel density estimation.

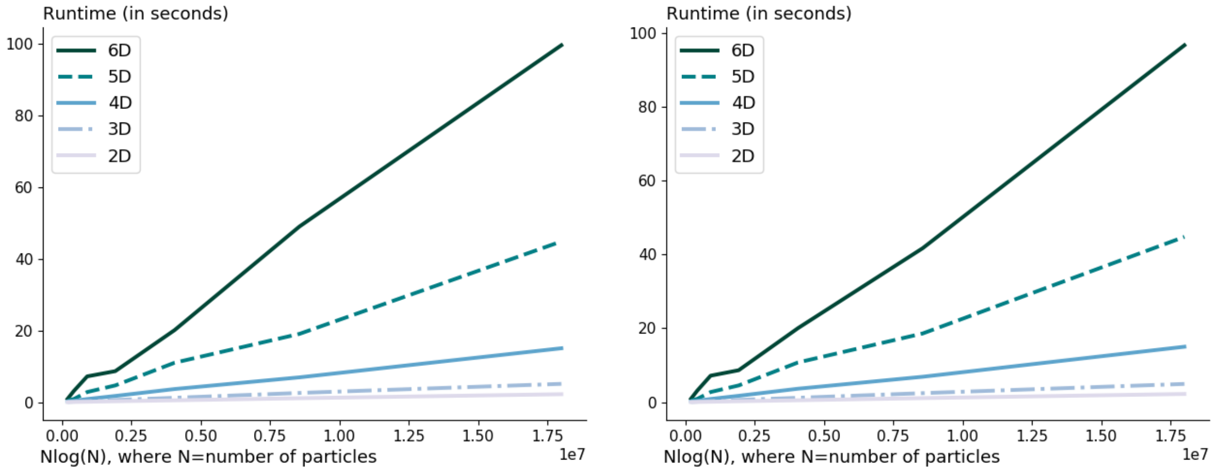

Figure 10: Runtime of fast kernel summation (left: bandwidth 15%; right: bandwidth 25%)

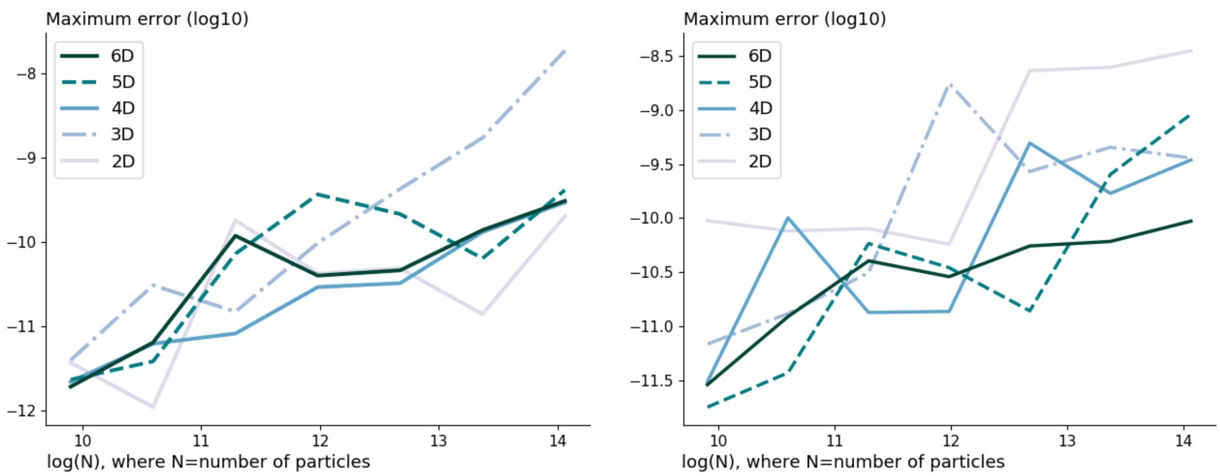

Figure 11: log 10 of maximum relative error w.r.t. log N (left: bandwidth 15%; right: 25%)

5. Conclusion

Fast and exact kernel density estimation can be achieved by the *fast sum updating* algorithm (Gasser and Kneip (1989), Seifert et al. (1994)). With N input points drawn from the density to estimate, and M evaluation points where this density needs to be estimated, the fast sum updating algorithm requires $\mathcal{O}(M \log M + N \log N)$ operations, which is a vast improvement over the $\mathcal{O}(MN)$ operations required by direct kernel summation. This paper revisits the fast sum updating algorithm and extends it in several ways.

The main contribution is the extension, for the first time, of the fast sum updating algorithm to the general multivariate case, opening the door to a vast class of practical density estimation and regression problems. The original concern in Seifert et al. (1994) with floating-point summation instability due to float-rounding errors can be completely addressed by the use of exact floating-point summation algorithms. Our numerical tests show that the cumulative float-rounding error is already negligible when using double-precision floats (in line with Fan and Marron (1994)), and that very simple compensated summation algorithms such as the Møller-Kahan algorithm can already bring significant accuracy improvements.

In addition, we show that fast sum updating is compatible with a larger list of kernels, including the triangular kernel, the Silverman kernel, the cosine kernel, and the newly introduced hyperbolic cosine kernel, than what was usually assumed in the literature. We introduce the multivariate additive kernel, which greatly improves the speed of fast sum updating in high dimension compared to product kernels. Importantly, we describe how fast sum updating is compatible with balloon adaptive bandwidths, and propose a fast approximate k-nearest-neighbor algorithm for the adaptive bandwidth.

The proposed multivariate extension does not impose any restriction on the input or output samples, but does require the evaluation points to lie on a possibly non-uniform grid. We describe how to prerotate the input data and construct a suitable grid to ease the interpolation of density estimates to any evaluation sample by multilinear interpolation or fast inverse distance weighting.

Our multivariate kernel density and locally linear regression tests confirm numerically the vastly improved computational speed compared to naive kernel summation, as well as the accuracy and stability of the method. A natural area for future research would be to examine density estimation or regression applications for which computational speed is a major issue. It would in particular be worth investigating how this algorithm compares, in terms of speed and accuracy, to alternative fast but approximate density estimation algorithms such as the Fast Fourier Transform with binning or the Fast Gauss Transform.

Acknowledgements

The authors are grateful to the anonymous referees for their valuable comments. Xavier Warin acknowledges the financial support of ANR project CAESARS (ANR-15-CE05-0024).

References

Boldo, S., S. Graillat, and J.-M. Muller (2017). On the robustness of the 2sum and fast2sum algorithms. *ACM Transactions on Mathematical Software 44*(1), 4:1–4:14. (Cited on page 7)

Bowman, A. and A. Azzalini (2003). Computational aspects of nonparametric smoothing with illustrations from the sm library. *Computational Statistics and Data Analysis 42*(4), 545–560. (Cited on page 2)

Chen, A. (2006). Fast kernel density independent component analysis. In *Independent Component Analysis and Blind Signal Separation*, Volume 3889 of *Lecture Notes in Computer Science*, pp. 24–31. Springer. (Cited on pages 2 and 33)

Curtin, R., W. March, R. P., D. Anderson, A. Gray, and C. Isbell Jr. (2013). Tree-independent dual-tree algorithms. In *Proceedings of the 30th International Conference on Machine Learning*, Volume 28, pp. 1435–1443. (Cited on page 3)

Demmel, J. and Y. Hida (2003). Accurate and efficient floating point summation. *SIAM Journal on Scientific Computing 25*(4), 1214–1248. (Cited on page 7)

Epanechnikov, V. (1969). Non-parametric estimation of a multivariate probability density. *Theory of Probability and its Applications 14*(1), 153–158. (Cited on page 4)

Fan, J. and J. Marron (1994). Fast implementation of nonparametric curve estimators. *Journal of Computational and Graphical Statistics 3*(1), 35–56. (Cited on pages 2, 29, and 35)

Fukunaga, K. and L. Hostetler (1975). The estimation of the gradient of a density function, with applications in pattern recognition. *IEEE Transactions on Information Theory 21*(1), 32–40. (Cited on page 9)

Gasser, T. and A. Kneip (1989). Discussion: linear smoothers and additive models. *The Annals of Statistics 17*(2), 532–535. (Cited on pages 2 and 28)

Gevret, H., N. Langrené, J. Lelong, X. Warin, and A. Maheshwari (2018). STochastic OPTimization library in C++. Technical report, EDF Lab. (Cited on page 22)

Gramacki, A. and J. Gramacki (2017). FFT-based fast computation of multivariate kernel density estimators with unconstrained bandwidth matrices. *Journal of Computational and Graphical Statistics 26*(2), 459–462. (Cited on page 2)

Gray, A. and A. Moore (2001). 'n-body' problems in statistical learning. In *Advances in Neural Information Processing Systems 13*, pp. 521–527. (Cited on page 3)

Gray, A. and A. Moore (2003). Nonparametric density estimation: Toward computational tractability. In *Proceedings of the SIAM International Conference on Data Mining*, pp. 203–211. (Cited on page 3)

Greengard, L. and J. Strain (1991). The Fast Gauss Transform. *SIAM Journal on Scientific and Statistical Computing 12*(1), 79–94. (Cited on pages 2 and 4)

Greengard, L. and X. Sun (1998). A new version of the Fast Gauss Transform. *Documenta Mathematica Extra Volume ICM III*, 575–584. (Cited on page 2)

Griebel, M. and D. Wissel (2013). Fast approximation of the discrete Gauss transform in higher dimensions. *Journal of Scientific Computing 55*(1), 149–172. (Cited on page 3)

Härdle, W. and M. Müller (2000). Multivariate and semiparametric kernel regression. In M. Schimek (Ed.), *Smoothing and regression*, pp. 357–391. Wiley. (Cited on page 9)

Härdle, W., M. Müller, S. Sperlich, and A. Werwatz (2004). *Nonparametric and Semiparametric Models*. Springer Series in Statistics. Springer. (Cited on page 2)

Hastie, T., R. Tibshirani, and J. Friedman (2009). *The Elements of Statistical Learning: Data Mining, Inference, and Prediction* (2nd ed.). Springer Series in Statistics. Springer. (Cited on page 2)

Higham, N. (1993). The accuracy of floating point summation. *SIAM Journal on Scientific Computing 14*(4), 783–799. (Cited on page 7)

Kahan, W. (1965). Pracniques: further remarks on reducing truncation errors. *Communications of the ACM 8*(1), 40. (Cited on page 7)

Lambert, C., S. Harrington, C. Harvey, and A. Glodjo (1999). Efficient on-line nonparametric kernel density estimation. *Algorithmica 25*(1), 37–57. (Cited on page 2)

Lang, D., M. Klaas, and N. de Freitas (2005). Empirical testing of fast kernel density estimation algorithms. Technical report, University of British Columbia. (Cited on page 3)

Lee, D., A. Moore, and A. Gray (2006). Dual-tree Fast Gauss Transforms. In *Advances in Neural Information Processing Systems 18*, pp. 747–754. (Cited on page 3)

Lee, D., P. Sao, R. Vuduc, and A. Gray (2014). A distributed kernel summation framework for general-dimension machine learning. *Statistical Analysis and Data Mining 7*(1), 1–13. (Cited on page 3)

Linnainmaa, S. (1974). Analysis of some known methods of improving the accuracy of floating-point sums. *BIT Numerical Mathematics 14*(2), 167–202. (Cited on pages 7, 22, and 35)

Loader, C. (1999). *Local Regression and Likelihood*. Statistics and Computing. Springer. (Cited on page 2)

Loftsgaarden, D. and C. Quesenberry (1965). A nonparametric estimate of a multivariate density function. *The Annals of Mathematical Statistics 36*(3), 1049–1051. (Cited on page 19)

McNamee, J. (2004). A comparison of methods for accurate summation. *ACM SIGSAM Bulletin 38*(1), 1–7. (Cited on page 7)

Møller, O. (1965). Quasi double-precision in floating-point addition. *BIT Numerical Mathematics 5*(1), 37–50. (Cited on pages 7, 22, and 35)

Morariu, V., B. Srinivasan, V. Raykar, R. Duraiswami, and L. Davis (2009). Automatic online tuning for fast Gaussian summation. In *Advances in Neural Information Processing Systems 21*, pp. 1113–1120. (Cited on page 2)

Neal, R. (2015). Fast exact summation using small and large superaccumulators. Technical report, University of Toronto. (Cited on page 7)

Ozawa, K. (1983). Analysis and improvement of Kahan's summation algorithm. *Journal of Information Processing 6*(4), 226–230. (Cited on pages 22 and 35)

Pan, V., B. Murphy, G. Qian, and R. Rosholt (2009). A new error-free floating-point summation algorithm. *Computers and Mathematics with Applications 57*(4), 560–564. (Cited on page 7)

Priest, D. (1991). Algorithms for arbitrary precision floating point arithmetic. In *Proceedings 10th IEEE Symposium on Computer Arithmetic*, pp. 132–143. (Cited on page 7)

Ram, P., D. Lee, W. March, and A. Gray (2009). Linear-time algorithms for pairwise statistical problems. In *Advances in Neural Information Processing Systems 22*, pp. 1527–1535. (Cited on page 3)

Raykar, V., R. Duraiswami, and L. Zhao (2010). Fast computation of kernel estimators. *Journal of Computational and Graphical Statistics 19*(1), 205–220. (Cited on page 2)

Rump, S., T. Ogita, and S. Oishi (2008). Accurate floating-point summation Part I: Faithful rounding. *SIAM Journal on Scientific Computing 25*(1), 189–224. (Cited on page 7)

Sampath, R., H. Sundar, and S. Veerapaneni (2010). Parallel Fast Gauss Transform. In *Proceedings of the IEEE International Conference for High Performance Computing, Networking, Storage and Analysis*. (Cited on page 2)

Scott, D. (1985). Averaged shifted histograms: effective nonparametric density estimators in several dimensions. *Annals of Statistics 13*(3), 1024–1040. (Cited on page 2)

Scott, D. (2014). *Multivariate density estimation: theory, practice and visualization* (2nd ed.). Wiley Series in Probability and Statistics. Wiley. (Cited on page 2)

Scott, D. and S. Sain (2005). Multivariate density estimation. In *Data Mining and Data Visualization*, Volume 24 of *Handbook of Statistics*, Chapter 9, pp. 229–261. Elsevier. (Cited on pages 18 and 19)

Seifert, B., M. Brockmann, J. Engel, and T. Gasser (1994). Fast algorithms for nonparametric curve estimation. *Journal of Computational and Graphical Statistics 3*(2), 192–213. (Cited on pages 2, 7, 28, and 33)

Shepherd, D. (1968). A two-dimensional interpolation function for irregularly-spaced data. In *Proceedings of the 1968 ACM National Conference*, pp. 517–524. (Cited on page 19)

Silverman, B. (1982). Algorithm AS 176: Kernel density estimation using the Fast Fourier Transform. *Journal of the Royal Statistical Society. Series C (Applied Statistics) 31*(1), 93–99. (Cited on pages 2 and 9)

Spivak, M., S. Veerapaneni, and L. Greengard (2010). The Fast Generalized Gauss Transform. *SIAM Journal on Scientific Computing 32*(5), 3092–3107. (Cited on page 2)

Terrell, G. and D. Scott (1992). Variable kernel density estimation. *The Annals of Statistics 20*(3), 1236–1265. (Cited on page 19)

Turlachand, B. and M. Wand (1996). Fast computation of auxiliary quantities in local polynomial regression. *Journal of Computational and Graphical Statistics 5*(4), 337–350. (Cited on page 2)

Wand, M. (1994). Fast computation of multivariate kernel estimators. *Journal of Computational and Graphical Statistics 3*(4), 433–445. (Cited on pages 2 and 18)

Wand, M. and M. Jones (1995). *Kernel Smoothing*. Chapman & Hall. (Cited on pages 7, 9, and 10)

Werthenbach, C. and E. Herrmann (1998). A fast and stable updating algorithm for bivariate nonparametric curve estimation. *Journal of Computational and Graphical Statistics 7*(1), 61–76. (Cited on pages 2 and 3)

Yang, C., R. Duraiswami, N. Gumerov, and L. Davis (2003). Improved Fast Gauss Transform and efficient kernel density estimation. In *Proceedings of the IEEE International Conference on Computer Vision*, pp. 464–471. (Cited on page 2)

Zhu, Y.-K. and W. Hayes (2010). Algorithm 908: Online exact summation of floating-point streams. *ACM Transactions on Mathematical Software 37*(3). (Cited on page 7)

A. Kernels compatible with fast sum updating

This Appendix details how to implement the fast sum updating algorithm for the kernels listed in Table 1. Three classes of kernels admit the type of separation between sources and targets required for the fast sum updating algorithm: polynomial kernels (subsection A.1), absolute kernels (subsection A.2) and cosine kernels (subsection A.3). In addition, fast sum updating is still applicable to kernels which combine features from these three classes (subsection A.4). In the literature, Seifert et al. (1994) covered the case of polynomial kernels, while Chen (2006) covered the Laplacian kernel. The present paper extends the applicability of fast sum updating to the triangular kernel, cosine kernel, hyperbolic cosine kernel, and combinations such as the tricube and Silverman kernels.

Specifically, we detail how to decompose the sums

$$\frac{1}{N}\sum_{i=1}^{N} K_h(x_i - z_j) x_i^p y_i^q = \frac{1}{Nh_j}\sum_{i=1}^{N} K\left(\frac{x_i - z_j}{h}\right) x_i^p y_i^q \, , \; j \in \{1, 2, \ldots, M\}$$

into fast updatable sums of the type

$$\mathcal{S}^{p,q}\left(f, [L, R]\right) := \sum_{i=1}^{N} f(x_i) x_i^p y_i^q \mathbb{1}\{L \le x_i \le R\} \tag{19}$$

Equation (19) is a generalization of the sum (6) used in Section 2 for the Epanechnikov kernel. The additional $f(x_i)$ term in the sum is necessary for such kernels as the cosine or Laplacian ones.

Whenever possible, we will use adaptive kernels $h = h_j$ (balloon estimator, cf. subsection 3.2). Some kernels, such as polynomial kernels, can combine adaptive bandwidths with fast sum updating, but some other kernels cannot, as explained in the subsections below.

A.1. Polynomial kernels

The class of polynomial kernels, in particular the class of symmetric beta kernels

$$K(u) = \frac{(1-u^2)^\alpha}{2^{2\alpha+1}\frac{\Gamma(\alpha+1)\Gamma(\alpha+1)}{\Gamma(2\alpha+2)}} \mathbb{1}\{|u| \le 1\}$$

includes several classical kernels: the uniform/rectangular kernel ($\alpha = 0$), the Epanechnikov/-parabolic kernel ($\alpha = 1$), the quartic/biweight kernel ($\alpha = 2$) and the triweight kernel ($\alpha = 3$). We recall from Section 2 how to decompose the Epanechnikov kernel $K(u) = \frac{3}{4}(1-u^2)\mathbb{1}\{|u| \le 1\}$. By expanding the square term:

$$\begin{aligned}
&\sum_{i=1}^{N} K\left(\frac{x_i - z_j}{h_j}\right) x_i^p y_i^q \mathbb{1}\left\{\left|\frac{x_i - z_j}{h_j}\right| \le 1\right\} \\
&= \frac{3}{4}\sum_{i=1}^{N}\left\{\left(1 - \frac{z_j^2}{h_j^2}\right) + \frac{2z_j}{h_j^2}x_i - \frac{1}{h_j^2}x_i^2\right\} x_i^p y_i^q \mathbb{1}\left\{z_j - h_j \le x_i \le z_j + h_j\right\} \\
&= \frac{3}{4}\left(1 - \frac{z_j^2}{h_j^2}\right)\mathcal{S}^{p,q}\left(1, [z_j - h_j, z_j + h_j]\right) + \frac{3}{4}\frac{2z_j}{h_j^2}\mathcal{S}^{p+1,q}\left(1, [z_j - h_j, z_j + h_j]\right) \\
&- \frac{3}{4}\frac{1}{h_j^2}\mathcal{S}^{p+2,q}\left(1, [z_j - h_j, z_j + h_j]\right)
\end{aligned}$$

The other kernels within this class can be decomposed in a similar manner by expanding the power terms.

A.2. Absolute kernels

The class of absolute kernels contains kernels based on the absolute value $|u|$, such as the triangular kernel and the Laplacian kernel.
For the triangular kernel, $K(u) = (1 - |u|)\mathbb{1}\{|u| \leq 1\}$ and

$$
\begin{aligned}
&\sum_{i=1}^{N} K\left(\frac{x_i - z_j}{h_j}\right) x_i^p y_i^q \mathbb{1}\left\{\left|\frac{x_i - z_j}{h_j}\right| \leq 1\right\} \\
&= \sum_{i=1}^{N}\left(1 - \frac{x_i - z_j}{h_j}\right) x_i^p y_i^q \mathbb{1}\left\{z_j \leq x_i \leq z_j + h_j\right\} + \sum_{i=1}^{N}\left(1 - \frac{z_j - x_i}{h_j}\right) x_i^p y_i^q \mathbb{1}\left\{z_j - h_j \leq x_i < z_j\right\} \\
&= \left(1 + \frac{z_j}{h_j}\right)\mathcal{S}^{p,q}\left(1, [z_j, z_j + h_j]\right) - \frac{1}{h_j}\mathcal{S}^{p+1,q}\left(1, [z_j, z_j + h_j]\right) \\
&+ \left(1 - \frac{z_j}{h_j}\right)\mathcal{S}^{p,q}\left(1, [z_j - h_j, z_j[\right) + \frac{1}{h_j}\mathcal{S}^{p+1,q}\left(1, [z_j - h_j, z_j[\right)
\end{aligned}
$$

For the Laplacian kernel, $K(u) = \frac{1}{2}\exp(-|u|)$ and

$$
\begin{aligned}
&\sum_{i=1}^{N} K\left(\frac{x_i - z_j}{h}\right) x_i^p y_i^q \\
&= \frac{1}{2}\sum_{i=1}^{N} \exp\left(-\frac{x_i - z_j}{h}\right) x_i^p y_i^q \mathbb{1}\left\{z_j \leq x_i\right\} + \frac{1}{2}\sum_{i=1}^{N} \exp\left(-\frac{z_j - x_i}{h}\right) x_i^p y_i^q \mathbb{1}\left\{x_i < z_j\right\} \\
&= \frac{1}{2}\exp\left(\frac{z_j}{h}\right)\mathcal{S}^{p,q}\left(\exp(-./h), [z_j, \infty[\right) + \frac{1}{2}\exp\left(-\frac{z_j}{h}\right)\mathcal{S}^{p,q}\left(\exp(./h),]-\infty, z_j[\right)
\end{aligned}
$$

where $\exp(\pm./h)$ denotes the function $u \mapsto \exp(\pm u/h)$. Remark that we used a constant bandwidth h, as neither a balloon bandwidth $h = h_j$ nor a sample point bandwidth $h = h_i$ can separate the term $\exp\left(\frac{x_i - z_j}{h}\right)$ into a product of a term depending on i only and a term depending on j only. Note that an intermediate adaptive bandwidth approach of the type $\frac{x_i}{h_i} - \frac{z_j}{h_j}$ would maintain the ability to separate sources and targets for this kernel.

A.3. Cosine kernels

For the cosine kernel, $K(u) = \frac{\pi}{4}\cos\left(\frac{\pi}{2}u\right)\mathbb{1}\{|u| \leq 1\}$ and

$$
\begin{aligned}
&\sum_{i=1}^{N} K\left(\frac{x_i - z_j}{h}\right) x_i^p y_i^q \mathbb{1}\left\{\left|\frac{x_i - z_j}{h}\right| \leq 1\right\} \\
&= \frac{\pi}{4}\sum_{i=1}^{N}\left\{\cos\left(\frac{\pi}{2}\frac{x_i}{h}\right)\cos\left(\frac{\pi}{2}\frac{z_j}{h}\right) + \sin\left(\frac{\pi}{2}\frac{x_i}{h}\right)\sin\left(\frac{\pi}{2}\frac{z_j}{h}\right)\right\} x_i^p y_i^q \mathbb{1}\left\{z_j - h \leq x_i \leq z_j + h\right\} \\
&= \frac{\pi}{4}\cos\left(\frac{\pi}{2}\frac{z_j}{h}\right)\mathcal{S}^{p,q}\left(\cos\left(\frac{\pi}{2}\frac{.}{h}\right), [z_j - h, z_j + h]\right) + \frac{\pi}{4}\sin\left(\frac{\pi}{2}\frac{z_j}{h}\right)\mathcal{S}^{p,q}\left(\sin\left(\frac{\pi}{2}\frac{.}{h}\right), [z_j - h, z_j + h]\right)
\end{aligned}
$$

where we used that $\cos(\alpha - \beta) = \cos(\alpha)\cos(\beta) + \sin(\alpha)\sin(\beta)$. In a similar manner, one can define a new kernel based on the hyperbolic cosine function

$$K(u) = \frac{1}{4 - 2\frac{\sinh(\log(2+\sqrt{3}))}{\log(2+\sqrt{3})}} \left\{2 - \cosh(\log(2+\sqrt{3})u)\right\} \mathbb{1}\{|u| \leq 1\}$$

and use the identity $\cosh(\alpha - \beta) = \cosh(\alpha)\cosh(\beta) - \sinh(\alpha)\sinh(\beta)$ to obtain a similar decomposition.

A.4. Combinations

Finally, one can combine the polynomial, absolute, and cosine approaches together to generate additional kernels compatible with fast sum updating. This combination approach contains the tricube kernel $K(u) = \frac{70}{81}(1 - |u|^3)^3 \mathbb{1}\{|u| \leq 1\}$ (polynomial + absolute value) and the Silverman kernel $K(u) = \frac{1}{2}\exp\left(-\frac{|u|}{\sqrt{2}}\right)\sin\left(\frac{|u|}{\sqrt{2}} + \frac{\pi}{4}\right)$ (absolute value + cosine). New kernels can be created by combining cosine kernels with polynomials, or the three approaches together. Obtaining the updating equations for these combined kernels is a straight application of the decomposition tools used in the previous subsections A.1, A.2 and A.3.

B. Stable fast sum updating

As observed in Fan and Marron (1994) and in the numerical section 4, the numerical rounding errors are invisible when using double-precision floating-point format. Nevertheless, it is possible to greatly reduce or remove altogether the residual floating-point rounding errors by implementing alternative summation algorithms, as discussed in subsection 2.2. As an illustration, Algorithm 5 below shows how to modify the univariate fast sum updating algorithm 1 to use the stable Møller-Kahan summation algorithm (Møller (1965), Linnainmaa (1974), Ozawa (1983)). The multivariate case can be adapted in a similar manner. Note that this stable version multiplies the computational effort by a constant, and in the multivariate case, the same is true of the memory consumption.

C. Multivariate kernel smoothers

In a multivariate setting, the kernel density estimator (1) becomes

$$\hat{f}_{\mathrm{KDE}}(z) := \frac{1}{N}\sum_{i=1}^{N} K_{d,H}(x_i - z) \tag{20}$$

where $x_i = (x_{1,i}, x_{2,i}, \ldots, x_{d,i})$, $i \in \{1, 2, \ldots, N\}$ are the input points, $z = (z_1, z_2, \ldots, z_d)$ is the evaluation point, and $K_{d,H}(u) = |H|^{-1/2} K_d(H^{-1/2}u)$ is a multivariate kernel with symmetric positive definite matrix bandwidth $H \in \mathbb{R}^{d\times d}$. Subsection 2.3.3 discusses the choice of kernel, and Condition 2 and subsection 3.2 discuss the possibility of adaptive bandwidth.

The multivariate version of the Nadaraya-Watson kernel regression estimator (2) is given by:

$$\hat{f}_{\mathrm{NW}}(z) := \frac{\sum_{i=1}^{N} K_{d,H}(x_i - z)y_i}{\sum_{i=1}^{N} K_{d,H}(x_i - z)} \tag{21}$$

Algorithm 5: Fast univariate kernel smoothing with stable Møller-Kahan summation

Input:
X: sorted vector of N inputs $X[1] \leq \ldots \leq X[N]$
Y: vector of N outputs $Y[1], \ldots, Y[N]$
Z: sorted vector of M evaluation points $Z[1] \leq \ldots \leq Z[M]$
H: vector of M bandwidths $H[1], \ldots, H[M]$
▷ Z and H should be such that the vectors Z-H and Z+H are increasing
iL = 1 ▷ The indices $1 \leq iL \leq iR \leq N$ will be such that the current bandwidth
iR = 1 ▷ $[Z[m] - H[m], Z[m] + H[m]]$ contains $X[iL], X[iL+1], \ldots, X[iR]$
$S[p_1, p_2] = 0$, $p_1 = 0, 1, \ldots, 4$, $p_2 = 0, 1$ ▷ Will contain the sum $\sum_{i=iL}^{iR} X[i]^{p_1} \times Y[i]^{p_2}$
$run[p_1, p_2] = 0$, $p_1 = 0, 1, \ldots, 4$, $p_2 = 0, 1$ ▷ running float-rounding error
for $m = 1, ..., M$ **do**
  while *(iR≤N) and (X[iR]<(Z[m]+H[m]))* **do**
    $aux[p_1, p_2] = X[iR]^{p_1} \times Y[iR]^{p_2} - run[p_1, p_2]$, $p_1 = 0, 1, \ldots, 4, p_2 = 0, 1$
    $temp[p_1, p_2] = S[p_1, p_2] + aux[p_1, p_2]$
    if *abs(S[p_1, p_2])>abs(aux[p_1, p_2])* **then**
      $run[p_1, p_2] = (temp[p_1, p_2] - S[p_1, p_2]) - aux[p_1, p_2]$
    else
      $run[p_1, p_2] = (temp[p_1, p_2] - aux[p_1, p_2]) - S[p_1, p_2]$
    end
    $S[p_1, p_2] = temp[p_1, p_2]$
    iR = iR + 1
  end
  while *(iL≤N) and (X[iL]<(Z[m]−H[m]))* **do**
    $aux[p_1, p_2] = -X[iL]^{p_1} \times Y[iL]^{p_2} - run[p_1, p_2]$, $p_1 = 0, 1, \ldots, 4, p_2 = 0, 1$
    $temp[p_1, p_2] = S[p_1, p_2] + aux[p_1, p_2]$
    if *abs(S[p_1, p_2])>abs(aux[p_1, p_2])* **then**
      $run[p_1, p_2] = (temp[p_1, p_2] - S[p_1, p_2]) - aux[p_1, p_2]$
    else
      $run[p_1, p_2] = (temp[p_1, p_2] - aux[p_1, p_2]) - S[p_1, p_2]$
    end
    $S[p_1, p_2] = temp[p_1, p_2]$
    iL = iL + 1
  end
  ▷ Here $S[p_1, p_2] = \sum_{i=iL}^{iR} X[i]^{p_1} Y[i]^{p_2}$, which can be used to compute
  ▷ $SK[p_1, p_2] = \sum_{i=iL}^{iR} X[i]^{p_1} Y[i]^{p_2} \; K(Z[m], X[i])$
  $C0 = 1.0 - Z[m]^2/H[m]^2$; $C1 = 2.0 \times Z[m]/H[m]^2$; $C2 = 1/H[m]^2$
  $SK[p_1, p_2] = C0 \times S[p_1, p_2] + C1 \times S[p_1 + 1, p_2] - C2 \times S[p_1 + 2, p_2]$
  $D[m] = 0.75 \times SK[0,0]/(H[m] \times N)$
  $R0[m] = SK[0,1]/SK[0,0]$
  $R1[m] = \begin{bmatrix} 1 & Z[m] \end{bmatrix} \begin{bmatrix} SK[0,0] & SK[1,0] \\ SK[1,0] & SK[2,0] \end{bmatrix}^{-1} \begin{bmatrix} SK[0,1] \\ SK[1,1] \end{bmatrix}$
end
return D, R0, R1

Output:
D[m]: kernel density estimate of X
R0[m]: locally constant regression of Y on X (kernel regression)
R1[m]: locally linear regression of Y on X
▷ The three estimates D[m], R0[m] and R1[m] are evaluated at point Z[m] with bandwidth H[m] and Epanechnikov kernel, for each m=1,... ,M

where y_i, $i \in \{1, 2, \dots, N\}$ are the output points. Finally, the multivariate version of the locally linear regression (3) is given by:

$$\hat{f}_{\mathrm{L}}(z) := \min_{\alpha(z), \beta_1(z), \dots, \beta_d(z)} \sum_{i=1}^{N} K_{d,H}(x_i - z) \left[y_i - \alpha(z) - \sum_{k=1}^{d} \beta_k(z) x_{k,i} \right]^2 \tag{22}$$

By solving the minimization problem (22), the multivariate locally linear regression estimate $\hat{f}_{\mathrm{L}}(z)$ is explicitly given by:

$$\hat{f}_{\mathrm{L}}(z) = \begin{bmatrix} 1 \\ z_1 \\ z_2 \\ \vdots \\ z_d \end{bmatrix}^T \begin{bmatrix} \sum_{i=1}^{N} K_{d,H}(z,x_i) & \sum_{i=1}^{N} x_{1,i} K_{d,H}(z,x_i) & \cdots & \sum_{i=1}^{N} x_{d,i} K_{d,H}(z,x_i) \\ \sum_{i=1}^{N} x_{1,i} K_{d,H}(z,x_i) & \sum_{i=1}^{N} x_{1,i} x_{1,i} K_{d,H}(z,x_i) & \cdots & \sum_{i=1}^{N} x_{1,i} x_{d,i} K_{d,H}(z,x_i) \\ \vdots & \vdots & \ddots & \vdots \\ \sum_{i=1}^{N} x_{d,i} K_{d,H}(z,x_i) & \sum_{i=1}^{N} x_{d,i} x_{1,i} K_{d,H}(z,x_i) & \cdots & \sum_{i=1}^{N} x_{d,i} x_{d,i} K_{d,H}(z,x_i) \end{bmatrix}^{-1} \begin{bmatrix} \sum_{i=1}^{N} y_i K_{d,H}(z,x_i) \\ \sum_{i=1}^{N} y_i x_{1,i} K_{d,H}(z,x_i) \\ \vdots \\ \sum_{i=1}^{N} y_i x_{d,i} K_{d,H}(z,x_i) \end{bmatrix} \tag{23}$$

To sum up, computing $\hat{f}_{\mathrm{KDE}}(z)$ requires one sum, computing $\hat{f}_{\mathrm{NW}}(z)$ requires two sums, and finally one can check that computing $\hat{f}_{\mathrm{L}}(z)$ requires a total of $(d+1)(d+4)/2$ sums.

Remark that this paper focuses on the three kernel smoothers (20), (21) and (23), but more general kernel smoothers can be implemented with the same fast multivariate sum updating algorithm described in this paper. For example, beyond the locally linear regression (23), one can consider locally quadratic or locally polynomial regressions. Another example is to use the matrices in (23) to implement more general regressions that ordinary least squares, for example penalized regressions such as locally linear Ridge regression or locally linear Lasso regression.

D. Fast bivariate sweeping algorithm

This Appendix illustrates the fast bivariate sweeping algorithm 2 with the help of Figures 12 and 13. As explained in subsection 2.3.6, we start from $j_1 = 1$ and $\mathcal{T}^{\mathrm{idx}}_{1,l_2} = \sum_{l_1=L_{1,1}}^{R_{1,1}} \mathcal{S}^{\mathrm{idx}}_{l_1,l_2}$ and iteratively increment j_1 and update $\mathcal{T}^{\mathrm{idx}}_{1,l_2}$ using equation (17). Figure 12 illustrates this fast sum updating in the first dimension. The partition contains $m_1 - 1 = 10$ columns and $m_2 - 1 = 6$ rows. Each rectangle in the partition is associated with its sum $\mathcal{S}^{\mathrm{idx}}_{l_1,l_2}$. On the left-side picture, the orange segment on each row l_2 corresponds to the sum $\sum_{l_1=L_{1,j_1-1}}^{R_{1,j_1-1}} \mathcal{S}^{\mathrm{idx}}_{l_1,l_2}$. The middle picture represents the fast sum updating (17): for each row l_2, the green sum $\sum_{l_1=R_{1,j_1-1}+1}^{R_{1,j_1}} \mathcal{S}^{\mathrm{idx}}_{l_1,l_2}$ is added to $\sum_{l_1=L_{1,j_1-1}}^{R_{1,j_1-1}} \mathcal{S}^{\mathrm{idx}}_{l_1,l_2}$ and the red sum $\sum_{l_1=L_{1,j_1-1}}^{L_{1,j_1}-1} \mathcal{S}^{\mathrm{idx}}_{l_1,l_2}$ is subtracted from it. The right-side picture show the result of the fast sum updating: the orange segment on each row l_2 corresponds to the updated sum $\sum_{l_1=L_{1,j_1}}^{R_{1,j_1}} \mathcal{S}^{\mathrm{idx}}_{l_1,l_2}$.

We next turn to the inner loop over j_2 and $\mathcal{T}^{\mathrm{idx}}_2$. In a similar manner, we start from $j_2 = 1$ and the initial sum $\mathcal{T}^{\mathrm{idx}}_2 = \sum_{l_2=L_{2,1}}^{R_{2,1}} \mathcal{T}^{\mathrm{idx}}_{1,l_2}$, and iteratively increment j_2 and update $\mathcal{T}^{\mathrm{idx}}_2$ using equation (18). Figure 13 illustrates this fast sum updating in the second dimension. On the left-side picture, for each row l_2, the orange segment is associated with its sum $\mathcal{T}^{\mathrm{idx}}_{1,l_2}$. The middle picture represents the fast sum updating (18): the green sum $\sum_{l_2=R_{2,j_2-1}+1}^{R_{2,j_2}} \mathcal{T}^{\mathrm{idx}}_{1,l_2}$ is added to $\sum_{l_2=L_{2,j_2}}^{R_{2,j_2}} \mathcal{T}^{\mathrm{idx}}_{1,l_2}$ and the red sum $\sum_{l_2=L_{2,j_2-1}}^{L_{2,j_2}-1} \mathcal{T}^{\mathrm{idx}}_{1,l_2}$ is subtracted from it. The right-hand side

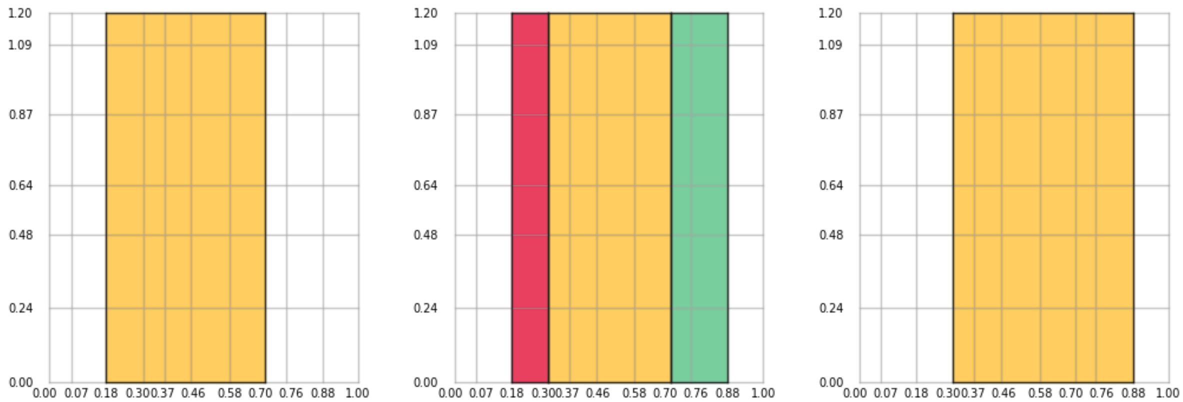

Figure 12: Bivariate fast sum updating: outer loop

picture show the result of this second fast sum updating: the orange hypercube is associated with the updated sum $\sum_{l_2=L_{2,j_2}}^{R_{2,j_2}} \mathcal{T}^{\text{idx}}_{1,l_2} = \sum_{l_1=L_{1,j_1}}^{R_{1,j_1}} \sum_{l_2=L_{2,j_2}}^{R_{2,j_2}} \mathcal{S}^{\text{idx}}_{l_1,l_2}$. Using Lemma 2.1 (equation (16)), this sum is equal to $\mathcal{S}^{\mathbf{p},q}_{\mathbf{k}}([z_j - h_j, z_j + h_j])$ which can be used to compute the kernel sums $\mathbf{S}_j = \mathbf{S}^{p_1,p_2,q}_{k_1,k_2,j}$ using equation (12), from which the bivariate kernel smoothers (kernel density estimator (20), kernel regression (21), locally linear regression (22)) can be computed.

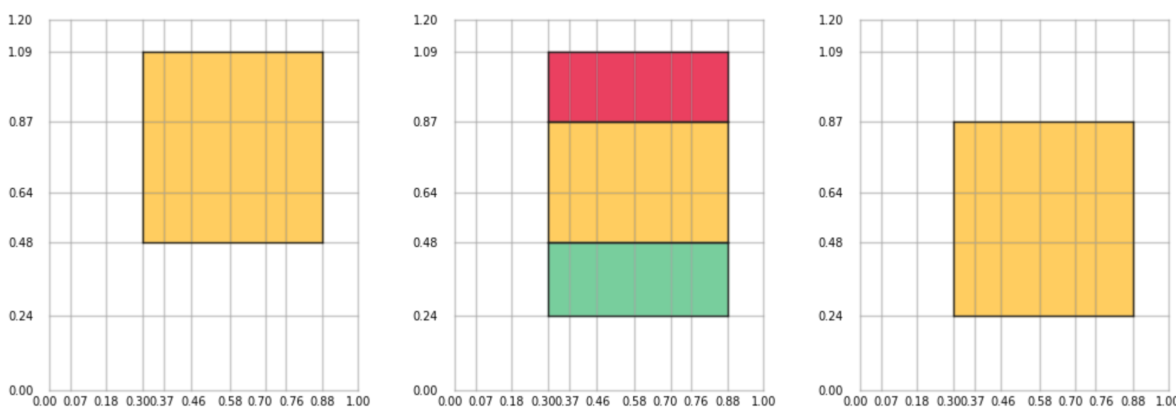

Figure 13: Bivariate fast sum updating: inner loop